

## Physicochemical and biological characterization of SB2, a biosimilar of Remicade® (infliximab)

Juyong Hong, Yuhwa Lee, Changsoo Lee, Suhyeon Eo, Soyeon Kim, Nayoung Lee, Jongmin Park, Seungkyu Park, Donghyuck Seo, Min Jeong, Youngji Lee, Soojeong Yeon, George Bou-Assaf, Zoran Susic, Wei Zhang & Orlando Jaquez

**To cite this article:** Juyong Hong, Yuhwa Lee, Changsoo Lee, Suhyeon Eo, Soyeon Kim, Nayoung Lee, Jongmin Park, Seungkyu Park, Donghyuck Seo, Min Jeong, Youngji Lee, Soojeong Yeon, George Bou-Assaf, Zoran Susic, Wei Zhang & Orlando Jaquez (2016): Physicochemical and biological characterization of SB2, a biosimilar of Remicade® (infliximab), mAbs, DOI: [10.1080/19420862.2016.1264550](https://doi.org/10.1080/19420862.2016.1264550)

**To link to this article:** <http://dx.doi.org/10.1080/19420862.2016.1264550>



© 2017 The Author(s). Published with license by Taylor & Francis Group, LLC© Juyong Hong, Yuhwa Lee, Changsoo Lee,



Accepted author version posted online: 22 Dec 2016.  
Published online: 22 Dec 2016.



Suhyeon Eo, Soyeon Kim, Nayoung Lee, Jongmin Park, Seungkyu Park, Donghyuck Seo, Min Jeong, Youngji Lee, Soojeong Yeon, George Bou-Assaf, Zoran Susic, Wei Zhang, and Orlando Jaquez



Article views: 279



View related articles ↗



View Crossmark data ↗

REPORT

 OPEN ACCESS

## Physicochemical and biological characterization of SB2, a biosimilar of Remicade® (infliximab)

Juyong Hong<sup>a</sup>, Yuhwa Lee<sup>a</sup>, Changsoo Lee<sup>a</sup>, Suhyeon Eo<sup>a</sup>, Soyeon Kim<sup>a</sup>, Nayoung Lee<sup>id a</sup>, Jongmin Park<sup>id a</sup>, Seungkyu Park<sup>a</sup>, Donghyuck Seo<sup>a</sup>, Min Jeong<sup>id a</sup>, Youngji Lee<sup>a</sup>, Soojeong Yeon<sup>a</sup>, George Bou-Assaf<sup>b</sup>, Zoran Susic<sup>b</sup>, Wei Zhang<sup>b</sup>, and Orlando Jaquez<sup>id c</sup>

<sup>a</sup>Quality Evaluation Team, Samsung Bioepis Co., Ltd, Incheon, South Korea; <sup>b</sup>Department of Analytical Development, Biogen, Inc., Cambridge, MA, USA; <sup>c</sup>Department of Medical Affairs, Biosimilars, Biogen, Zug, Switzerland

### ABSTRACT

A biosimilar is a biological medicinal product that contains a version of the active substance of an already authorized original biological medicinal product. Biosimilarity to the reference product (RP) in terms of quality characteristics, such as physicochemical and biological properties, safety, and efficacy, based on a comprehensive comparability exercise needs to be established. SB2 (Flixabi® and Renflexis®) is a biosimilar to Remicade® (infliximab). The development of SB2 was performed in accordance with relevant guidelines of the International Conference on Harmonisation, the European Medicines Agency, and the United States Food and Drug Administration. To determine whether critical quality attributes meet quality standards, an extensive characterization test was performed with more than 80 lots of EU- and US-sourced RP. The physicochemical characterization study results revealed that SB2 was similar to the RP. Although a few differences in physicochemical attributes were observed, the evidence from the related literature, structure-activity relationship studies, and comparative biological assays showed that these differences were unlikely to be clinically meaningful. The biological characterization results showed that SB2 was similar to the RP in terms of tumor necrosis factor- $\alpha$  (TNF- $\alpha$ ) binding and TNF- $\alpha$  neutralization activities as a main mode of action. SB2 was also similar in Fc-related biological activities including antibody-dependent cell-mediated cytotoxicity, complement-dependent cytotoxicity, neonatal Fc receptor binding, C1q binding, and Fc gamma receptor binding activities. These analytical findings support that SB2 is similar to the RP and also provide confidence of biosimilarity in terms of clinical safety and efficacy.

**Abbreviations:** Two-AB, 2-aminobenzamide; ADA, anti-drug antibody; ADCC, antibody-dependent cell-mediated cytotoxicity; CD, circular dichroism; CDC, complement-dependent cytotoxicity; CE-SDS, capillary electrophoresis-sodium dodecyl sulfate; CEX, cation exchange chromatography; CEX-HPLC, cation exchange-high-performance liquid chromatography Chinese hamster ovary; CPB, carboxypeptidase B; CQA, critical quality attribute; Sm, coefficient of sedimentation; DSC, differential scanning calorimetry; ELISA, enzyme-linked immunosorbent assay; EMA, European Medicines Agency; EU, European Union; Fc $\gamma$ R, Fc $\gamma$  receptors; FcRn, neonatal Fc receptor; FDA, Food and Drug Administration; FTIR, Fourier transform infrared spectroscopy; HDX, hydrogen/deuterium exchange; HILIC-UPLC, hydrophilic interaction ultra-performance liquid chromatography; HMW, high molecular weight; icIEF, imaging capillary isoelectric focusing; IgG, immunoglobulin G; ITF, intrinsic fluorescence; LC-ESI-MS, liquid chromatography-electrospray ionization-mass spectrometry; LC-ESI-MS/MS, liquid chromatography-electrospray ionization-tandem mass spectrometry; LMW, low molecular weight; MALLS, multi-angle laser light scattering; MOA, mode of action; MS, mass spectrometry; MS/MS, tandem mass spectrometry; NANA, N-acetylneuraminic acid; NGNA, N-glycolylneuraminic acid; OD<sub>d</sub>, optical density difference; PBMcs, peripheral blood mononuclear cells; RP, reference product; SAR, structure-activity relationship; SEC, size-exclusion chromatography; SEC/MALLS, size-exclusion chromatography coupled to multi-angle laser light scattering; SEC/UV, size-exclusion chromatography coupled to UV detector; SPR, surface plasmon resonance; SV-AUC, sedimentation velocity analytical ultracentrifugation; TNF- $\alpha$ , tumor necrosis factor  $\alpha$ ; UPLC, ultra-performance liquid chromatography; US, United States; UV, ultraviolet.

### ARTICLE HISTORY

Received 27 July 2016  
Revised 9 November 2016  
Accepted 20 November 2016

### KEYWORDS

Biosimilar; critical quality attribute; flixabi; infliximab; renflexis; SB2

### Introduction

The loss of patent protection for some of the first “complex biologics” (e.g., monoclonal antibodies and Fc-fusion proteins) to be marketed has ushered in a new generation of biosimilars.<sup>1</sup> Since 2006, when the European Medicines Agency (EMA) began approving first-generation biosimilars of simpler

biologics,<sup>2</sup> such as somatropin, filgrastim, and epoietin,<sup>3</sup> a growing number of biosimilars of complex biologics, such as monoclonal antibodies, have been approved in Europe and the United States. In 2013, CT-P13<sup>4</sup> became the first monoclonal antibody biosimilar to be recommended for approval by EMA’s Committee for Medicinal Products for Human Use, and

**CONTACT** Juyong Hong  [juyong.hong@samsung.com](mailto:juyong.hong@samsung.com)  Samsung Bioepis Co., Ltd., 107, Cheomdan-daero, Yeonsu-gu, Incheon 21987, Republic of Korea.

Published with license by Taylor and Francis Group, LLC © Samsung Bioepis

This is an Open Access article distributed under the terms of the Creative Commons Attribution-Non-Commercial License (<http://creativecommons.org/licenses/by-nc/3.0/>), which permits unrestricted non-commercial use, distribution, and reproduction in any medium, provided the original work is properly cited. The moral rights of the named author(s) have been asserted.

authorized by the European Commission as a biosimilar to Remicade®. It was closely followed by the approval of SB4<sup>5</sup> as the first biosimilar to Enbrel® in 2015, and in 2016, by the approval of SB2<sup>6</sup> as a second biosimilar to Remicade®.

A biosimilar is a biological medicinal product whose active substance is similar to that of an already approved original biological product.<sup>7,8,9</sup> Biosimilars must demonstrate similar physicochemical and biological characteristics, efficacy, and safety in accordance with the approval requirements of regulatory authorities such as the EMA and the US Food and Drug Administration (FDA).<sup>8</sup> According to US regulations, a biosimilar must be highly similar to its reference product (RP) “notwithstanding minor differences in clinically inactive components and without clinically meaningful differences in terms of safety, purity, and potency.”<sup>9</sup> Therefore, a series of comparability exercises should be performed to evaluate both similarities and differences in quality attributes between a biosimilar and its RP.

As a biosimilar to Remicade®, SB2 was developed and manufactured using Chinese hamster ovary (CHO) cell lines instead of the murine cell line (SP2/0) that was used for the production of Remicade®. We assessed the similarity of SB2 by extensive analyses and statistical comparison with more than 80 lots of EU-sourced and US-sourced RP, which enabled definition of the target quality product profile of infliximab. As we have stated previously,<sup>10</sup> analytical similarity studies should include similarity ranges based on data for the RP’s critical quality attributes (CQAs) that could potentially affect potency, efficacy, and safety, as well as for non-CQAs that are related to process consistency. Therefore, during the development and characterization of SB2, we determined Remicade®’s CQAs on the basis of the RP’s mode of action (MOA) and results from several structure-activity relationship (SAR) studies, using state-of-the-art and orthogonal methods. In the analytical similarity studies, all the possible quality attributes of SB2 were compared with those of the RP in analyses using more than 60 analytical methods; similarity ranges were based on 18 of these test methods.

Infliximab is a genetically engineered chimeric (human-murine) monoclonal antibody that consists of two light and two heavy chains and has an approximate molecular weight of 149 kDa.<sup>11,12</sup> Each light chain is composed of 214 amino acids with 5 cysteine residues and each heavy chain is composed of 450 amino acids with 11 cysteine residues.<sup>11</sup> All cysteine residues in the light and heavy chain are involved in either intra- or inter-disulfide bonds (Fig. 1). Infliximab binds with high affinity to tumor necrosis factor- $\alpha$  (TNF- $\alpha$ ) and thus blocks some of this cytokine’s effects, which include mediation of inflammatory responses and modulation of the immune system.<sup>12</sup> Evidence indicates that TNF- $\alpha$  plays an important role in autoimmune and inflammatory diseases. Remicade® is currently approved for use in the treatment of rheumatoid arthritis, adult Crohn’s disease, pediatric Crohn’s disease, ulcerative colitis, pediatric ulcerative colitis, psoriasis, psoriatic arthritis, and ankylosing spondylitis in the US.<sup>12</sup>

SB2 was developed as a biosimilar to Remicade® in accordance with the International Conference on Harmonisation of Technical Requirements for Registration of Pharmaceuticals for Human Use, the EMA, and the US FDA guidances regarding biosimilar and biotechnology/biological products. These documents provide information about test procedures and acceptance criteria for

biotechnological/biological products<sup>13</sup> and discuss quality considerations for similarity assessment.<sup>14,15</sup> CQAs of infliximab are highly related not only to its TNF- $\alpha$  binding and the corresponding neutralization effect of that binding, but also to its effector functions associated with the Fc domain (e.g., complement-dependent cytotoxicity [CDC] and antibody-dependent cell-mediated cytotoxicity [ADCC]). Here, we report the results of a subset (Table 1) of more than 60 structural, physicochemical, and biological analyses, which themselves representing a subset of the total comparability campaign of analyses, demonstrating the similarity between SB2 and its RP.

## Results

### Primary structure and disulfide linkages

EMA and FDA guidelines state that the amino acid sequences of the proposed biosimilar drug and of RP should be identical.<sup>14,16,17</sup> However, differences may exist in terminal amino acid sequences and post-translational modifications because of differences in proprietary expression systems, bioprocess, purification, formulation, and storage conditions.<sup>18</sup>

To compare the structural integrity of SB2 and RP, full amino acid sequences, and N- and C-terminal sequences were analyzed by liquid chromatography-electrospray ionization-tandem mass spectrometry (LC-ESI-MS/MS) peptide mapping. Experiments were performed with SB2 and RP in a side-by-side manner.

High similarity in peak intensities and retention times were observed in mirror images of the peptide chromatograms of Lys-C-digested SB2 and RP (Fig. 2A). When SB2 and RP chromatograms were compared, there were no new peaks for SB2. Sequencing of peptides generated by three enzymes (i.e., trypsin, Lys-C, and Asp-N, Fig. 2B) and accurate mass determination by complete or partial tandem mass spectrometry (MS/MS) data demonstrated that the amino acid sequences of SB2 and RP were identical. Sequence coverage of 100% was accomplished by these analyses (data not shown).

Analyzing peptides digested by trypsin, we conducted disulfide mapping of SB2 and RP under non-reducing and reducing conditions. All disulfide-linked peptides except one (i.e., a peptide in which the two heavy chain fragments were linked by two disulfide bonds at T21) were linked via one disulfide bond (Fig. 3 and Table 2). Two peptides, H: T20-L: T19 and H: T21 = H: T21, were linked by inter-chain disulfide bonds between the heavy and light chains and between the heavy chains. Total ion chromatograms of SB2 and RP were identical, showing that all 32 cysteine residues are linked by disulfide bonds and those identical sets of disulfide-bonded peptides were derived from RP. The results of these analyses demonstrated that the primary structure and disulfide linkages of SB2 and of RP were identical.

N- and C-terminal sequences obtained by peptide mapping showed that the N terminus of SB2 was identical to that of RP (data not shown), whereas differences were observed at the C terminus of the heavy chain. This analysis detected three C-terminal variants: the main C-terminal form, which lacked Lys (-SLSLSPG-449); a C-terminal form with  $\alpha$ -amidation (-SLSLSPamidated-448); and a C-terminal form with Lys (-SLSLSPGK-450) (data not shown). The C-terminal form lacking Lys was the most abundant heavy chain C-terminal variant

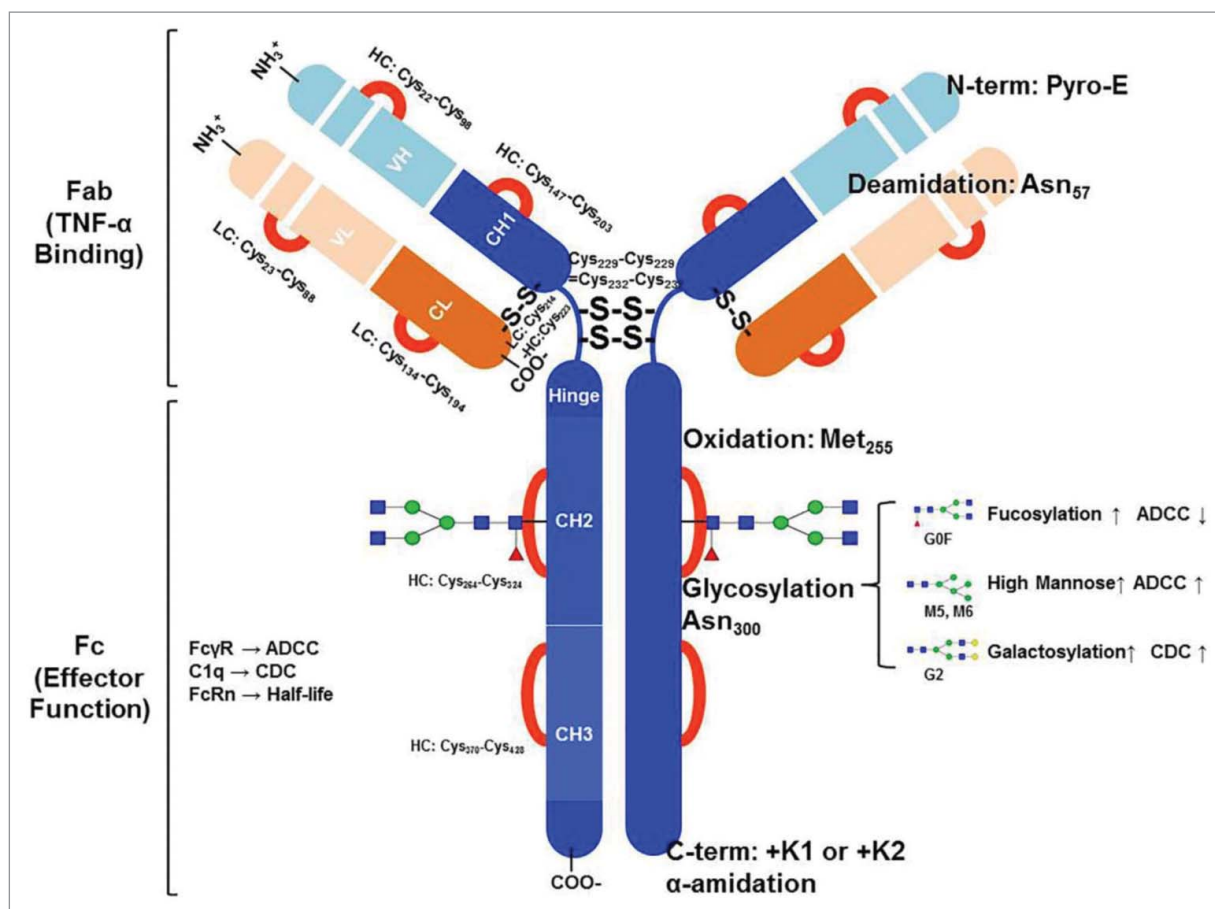


Figure 1. Schematic Structure of Infliximab.

for both products. However, the proportion of the SB2 C-terminal form with Lys was much lower than that of RP, and the C-terminal form with  $\alpha$ -amidation was only observed in SB2. These differences were considered to be mainly due to the use of CHO cells, instead of SP2/0 cells (used by the manufacturer of the RP), as host cells.<sup>19</sup> These results showed the correlation with the SB2 and RP charge patterns with and without treatment of carboxypeptidase B (CPB), detected by imaging capillary isoelectric focusing (icIEF) and cation exchange high-performance liquid chromatography (CEX-HPLC). The lack of impact of these differences on the purity, efficacy, and safety of SB2 is discussed below.

Additional sequence variants that resulted from post-translational modifications were identified by LC-ESI-MS/MS. The relative deamidation level of SB2 was highly similar to RP, but the relative oxidation level of residue Met<sub>255</sub>, which is susceptible to oxidation, was slightly higher in SB2 than in RP (data not shown). However, the difference was minor in quantity, and a SAR study based on charge variants isolation using CEX-HPLC showed that the oxidation of Met<sub>255</sub> had no substantial effect on biological activity (TNF- $\alpha$  and Fc $\gamma$ IIIa binding activities). Hence, the difference in Met<sub>255</sub> oxidation level between SB2 and RP was not considered to be functionally significant.

### Molecular weight

The molecular weights of intact SB2 and RP were measured by LC-ESI-MS under reducing and non-reducing conditions; the

same method was used to measure the molecular weights of deglycosylated SB2 and RP. The average masses of intact SB2 ( $148,517 \pm 2$  Da for 2H2L + 2G0F) and RP ( $148,515 \pm 2$  Da for 2H2L + 2G0F) were identical, considering assay variability (0.01% of theoretical mass). Under reducing conditions, the light chain masses of SB2 (23,435 Da) and RP (23,435 Da) were identical and consistent with the theoretical mass deduced from the gene sequence of infliximab. In addition, the heavy chain masses of SB2 ( $50,826 \pm 1$  Da for 1H + G0F) and RP ( $50,826 \pm 1$  Da for 1H + G0F) were identical. The masses of deglycosylated SB2 and RP under reducing and non-reducing conditions were also identical and consistent with the theoretical mass deduced from the gene sequence of infliximab (data not shown).

### Higher-order structures

Regulatory agencies have increasingly recommended state-of-the-art and orthogonal methodologies be used for demonstration of structural similarity between a biosimilar and its RP.<sup>20</sup> Accordingly, we conducted secondary and tertiary structural analysis using far- and near-UV (UV) circular dichroism (CD), intrinsic fluorescence (ITF), Fourier transform infrared spectroscopy (FTIR), and differential scanning calorimetry (DSC). While CD and FTIR can be used to reliably evaluate secondary and tertiary structures of relatively small proteins, large, complex, and heterogeneous biologics such as antibodies or Fc fusion proteins must be folded into proper 3-dimensional

**Table 1.** Summarized attributes and key findings.

Category	Product Quality Attributes	Analytical Methods	Assessment
	<b>Physicochemical characterization</b>		
<b>Primary Structure</b>	Molecular weight	Intact mass under reducing/non-reducing conditions	Similar to RP
	Amino acid sequence	Peptide mapping by LC-ESI-MS/MS using a combination of digestion enzymes	Similar to RP
	Terminal sequence		
	Methionine oxidation		
	Deamidation		
	C-terminal and N-terminal variants		
Disulfide linkage mapping	peptide mapping under non-reducing condition	Similar to RP	
<b>Higher-order Structure</b>	Protein secondary and tertiary structure	Far- and near-UV CD spectroscopy, ITF, HDX-MS, Antibody conformational array, DSC	Similar to RP Similar to RP Similar to RP
	<b>Glycosylation</b>	N-linked glycosylation site determination	LC-ESI-MS/MS
N-glycan identification		Procainamide labeling and LC-ESI-MS/MS	Minor differences were observed, but not clinically meaningful
	N-glycan profile analysis	2-AB labeling and HILIC-UPLC	Similar in terms of %Afucose+%HM and %Gal, %Charged glycans of SB2 is lower, but not clinically meaningful
<b>Aggregation</b>	Soluble aggregates	SEC-UV, SEC-MALLS/RI SV-AUC	Slightly higher compared with RP in HMW analyzed by SEC/UV, but SV-AUC and SEC-MALLS profiles of SB2 was similar to that of RP
<b>Fragmentation</b>	Low molecular weight	Non-reduced CE-SDS Reduced CE-SDS	Similar to RP
<b>Charge heterogeneity</b>	Acidic variants	CEX-HPLC and icIEF	Similar to RP
	Basic variants		Lower compared with RP, but not clinically meaningful
	<b>Biological Characterization</b>		
<b>Fab-related Biological Activity</b>	TNF- $\alpha$ neutralization activity	TNF- $\alpha$ neutralization assay by NF- $\kappa$ B reporter gene assay	Similar to RP
	TNF- $\alpha$ binding activity	FRET	Similar to RP
	Apoptosis activity	Cell-based assay	Similar to RP
	Transmembrane TNF- $\alpha$ binding assay	FACS	Similar to RP
<b>Fc-related Biological Activity</b>	FcRn binding	AlphaScreen <sup>®</sup>	Similar to RP
	Fc $\gamma$ R1IIa (V/V type) binding	SPR	Similar to RP
	ADCC using healthy donor PBMC	Cell-based assay	Similar to RP
	CDC	Cell-based assay	Similar to RP
	C1q binding	ELISA	Similar to RP
	Fc $\gamma$ R1a binding	FRET	Similar to RP
	Fc $\gamma$ R1IIa binding	SPR	Similar to RP
	Fc $\gamma$ R1IIb binding	SPR	Similar to RP
	Fc $\gamma$ R1IIIb binding	SPR	Similar to RP

Two-AB, 2-aminobenzamide; ADCC, antibody-dependent cell-mediated cytotoxicity; CD, circular dichroism; CDC, complement-dependent cytotoxicity; CE-SDS, capillary electrophoresis-sodium dodecyl sulfate; CEX-HPLC, cation exchange-high-performance liquid chromatography; DSC, differential scanning calorimetry; ELISA, enzyme-linked immunosorbent assay; FACS, fluorescence-activated cell sorting; FcRn, neonatal Fc receptors; FRET, fluorescence resonance energy transfer; HILIC-UPLC, hydrophilic interaction liquid chromatography-ultra-performance liquid chromatography; icIEF, imaging capillary isoelectric focusing; ITF, intrinsic fluorescence spectroscopy; LC-ESI-MS, liquid chromatography-electrospray ionization-mass spectrometry; LC/MS, liquid chromatography-mass spectrometry; LC-ESI-MS/MS liquid chromatography-electrospray ionization-tandem mass spectrometry; MFI, micro-flow imaging; PBMC, peripheral blood mononuclear cells; SEC, size exclusion chromatography; SEC-MALLS/RI, size exclusion chromatography-multi-angle laser light scattering/refractive index; SPR, surface plasmon resonance; SV-AUC, sedimentation velocity analytical ultracentrifugation; TNF, tumor necrosis factor; UV/VIS, UV visible.

structures to be functional; therefore, they are too complex for their secondary structures to be analyzed by these methods. DSC has proved to be useful for characterization of thermal stability, overall conformation, and folding integrity for these more complex biologics. The results of these structural analyses showed that the two products were highly similar (Fig. 4).

Hydrogen/deuterium exchange (HDX) and antibody conformational arrays were used for in-depth comparisons of the overall protein conformations of the two products. HDX combined with MS can characterize the solvent accessibility around a molecule's surface. This accessibility reflects the overall structural conformation and dynamics. HDX/MS can provide reliable comparative information that is independent of protein size. As such, HDX/MS is

considered one of the most sensitive and informative methods to evaluate similarity in higher order structure.<sup>21</sup> Amide hydrogens of the protein backbone exchange for deuterium during the incubation in D<sub>2</sub>O, and the exchange rate is determined at the peptide level on the local structure. After the exchange reaction is quenched, the protein is digested and the resulting peptides are separated and analyzed by LC-ESI-MS. Every time a deuterium replaces hydrogen on the peptide backbone, the mass of this peptide increases by 1 Da.

Butterfly plots of the HDX analysis showed almost perfect symmetry in the dynamics of deuterium uptake between SB2 and RP (Fig. 5A for heavy chain and Fig. 5B for light chain). This result demonstrates that SB2 and RP have highly similar

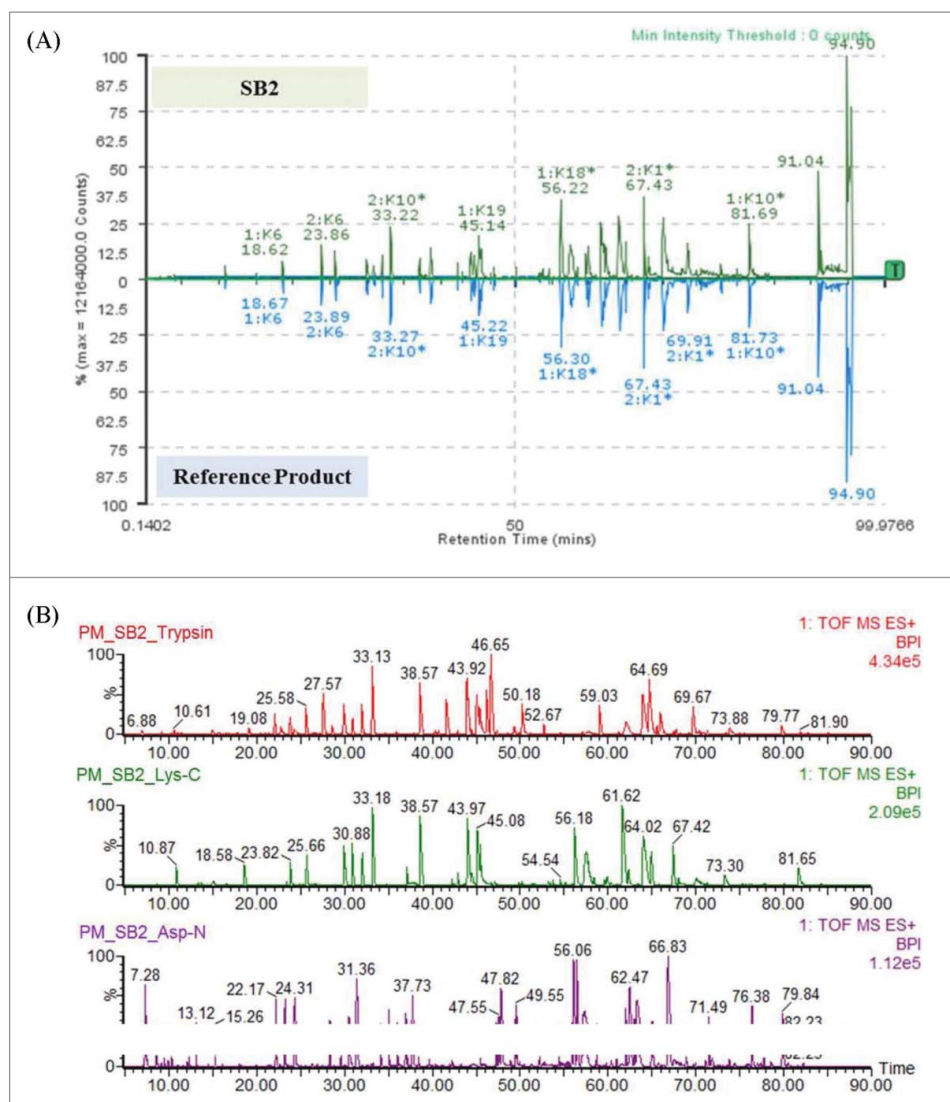


**Figure 2.** Primary Structure (Amino Acid Sequence) of SB2 and RP. (A) Mirror images of chromatograms of Lys-C-generated peptides of SB2 and RP. (B) Peptide maps of SB2 resulting from digestion with trypsin, Lys-C, and Asp-N.

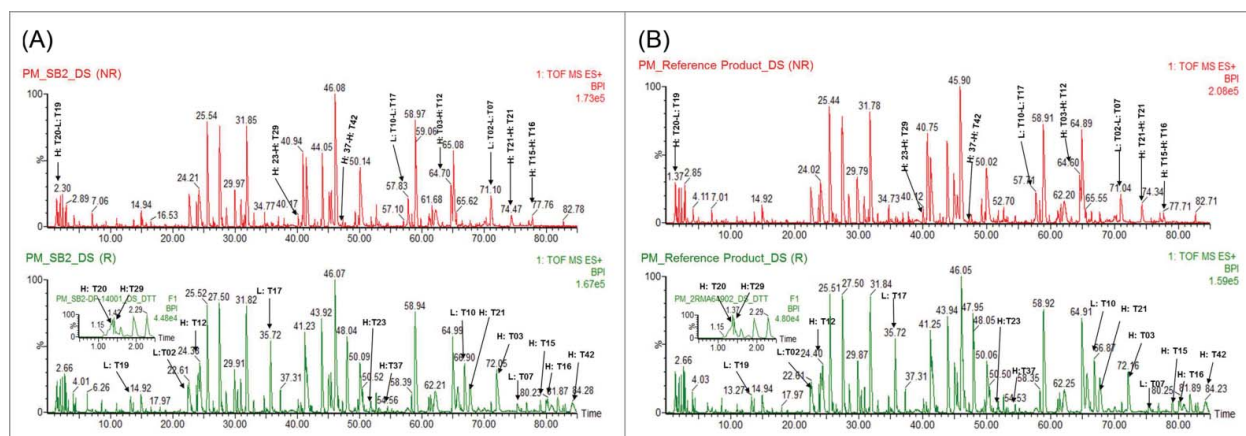


**Figure 3.** Peptide Maps of SB2 and RP under Non-reduced and Reduced Conditions. (A) Non-reduced (upper panels) and reduced (lower panels) peptide maps of SB2. (B) Non-reduced (upper panels) and reduced (lower panels) peptide maps of RP.

**Table 2.** Disulfide-linked peptide map.

Region	Type	Disulfide-Linked Peptides	No. of Disulfide Bond	Expected $m/z$ (Charge State)	Experimentally Detected $m/z$	
					SB2	RP
H	Intra-chain	H:Cys22-H:Cys98 (H:T3-H:T12)	1	886.90 (4)	886.90	886.90
		H:Cys147-H:Cys203 (H:T15-H:T16)	1	1132.00 (7)	1131.99	1131.99
		H:Cys264-H:Cys324 (H:T23-H:T29)	1	777.04 (3)	777.04	777.04
		H:Cys370-H:Cys428 (H:T37-H:T42)	1	769.97 (5)	769.97	769.97
		L:Cys23-L:Cys88 (L:T2-L:T7)	1	1141.71 (5)	1141.72	1141.72
L		L:Cys134-L:Cys194 (L:T10-L:T17)	1	712.16 (5)	712.16	712.16
H and L	Inter-chain	H:Cys223-L:Cys214 (H:T20-L:T19)	1	757.25 (1)	757.25	757.25
Hinge region		H:Cys229-Cys229=H:Cys232-Cys232 (H:T21 = H:T:21)	2	780.26 (7)	780.27	780.27

Abbreviations: H, heavy chain; L, light chain; T, tryptic peptide.

solvent accessibility over the incubation times from 0 to 240 minutes. Kinetic curves can be used to show the individual uptake rates of representative peptides from SB2 and RP (Fig. 5C for the heavy chain and Fig. 5D for the light chain). An analysis of 147 peptides representing coverage of 90.9% of the SB2 heavy chain sequence, including the sequences of multiple glycosylated peptides, and 69 peptides representing coverage of 98.6% of the SB2 light chain sequence yielded kinetic curves overlapping those of RP, a selection of which are presented in Fig. 5C for the heavy chain and Fig. 5D for the light chain. The differences between the products were not more than 1 Da across the entire sequence representing the heavy and light chain. These findings showed that the Fab and Fc conformations

of SB2 are highly similar to those of RP. These results are closely related to those of the Fab and Fc biological assays.

Antibody conformational arrays can also reveal reliable comparative information about protein conformation.<sup>22</sup> The results of the conformational antibody array are shown in Fig. 6 as a histogram, according to the extent of epitope exposure in the variable region. A total of 34 antibodies were used to detect regional changes in the 3-dimensional structure; 12 antibodies for Fab region and 22 antibodies for Fc regions. The results showed that the extent of epitope exposure of SB2 and RP was similar in the conformation of Fab region within the variability of the assay (Fig. 6) as well as Fc region. In addition, the calculated optical density difference ( $OD_d$ ) for SB2 was less

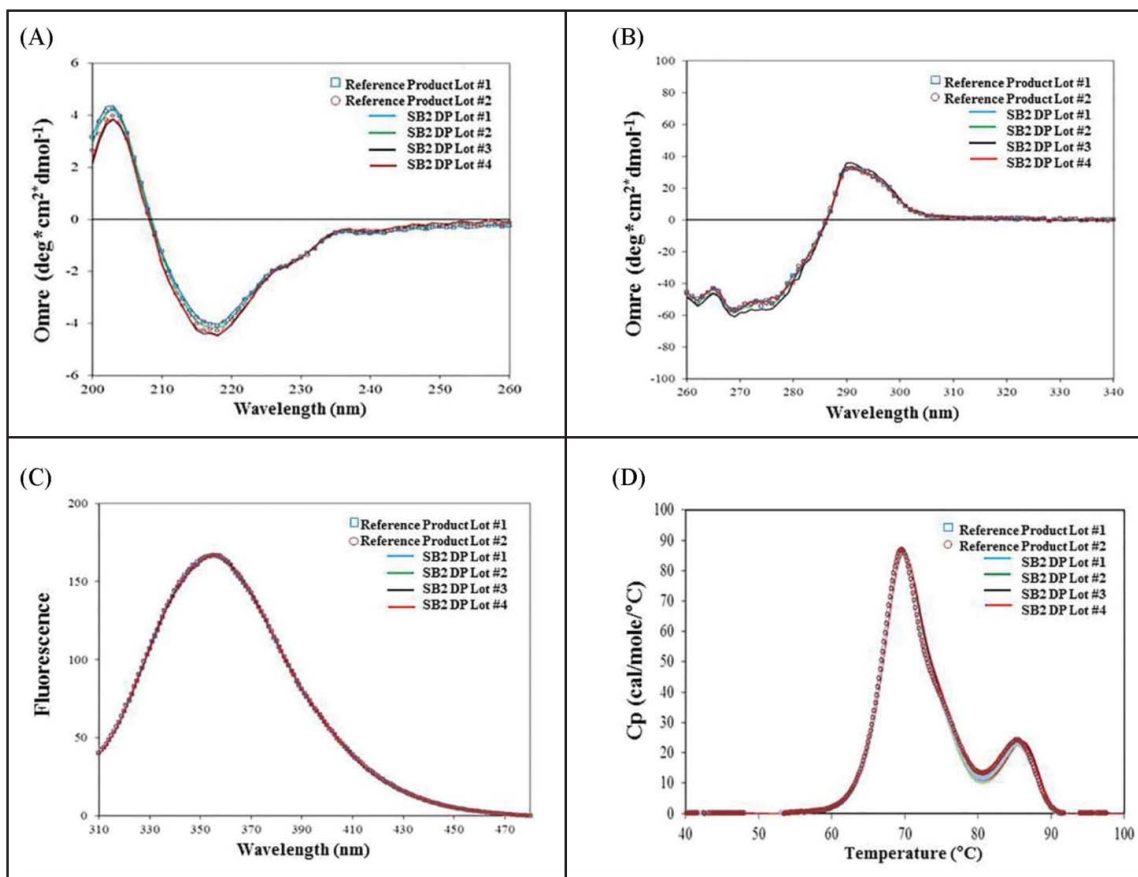


**Figure 4.** Higher-order Structures of SB2 and RP. (A) Far-UV CD spectra. (B) Near-UV CD spectra. (C) Intrinsic fluorescence. (D) DSC thermograms.

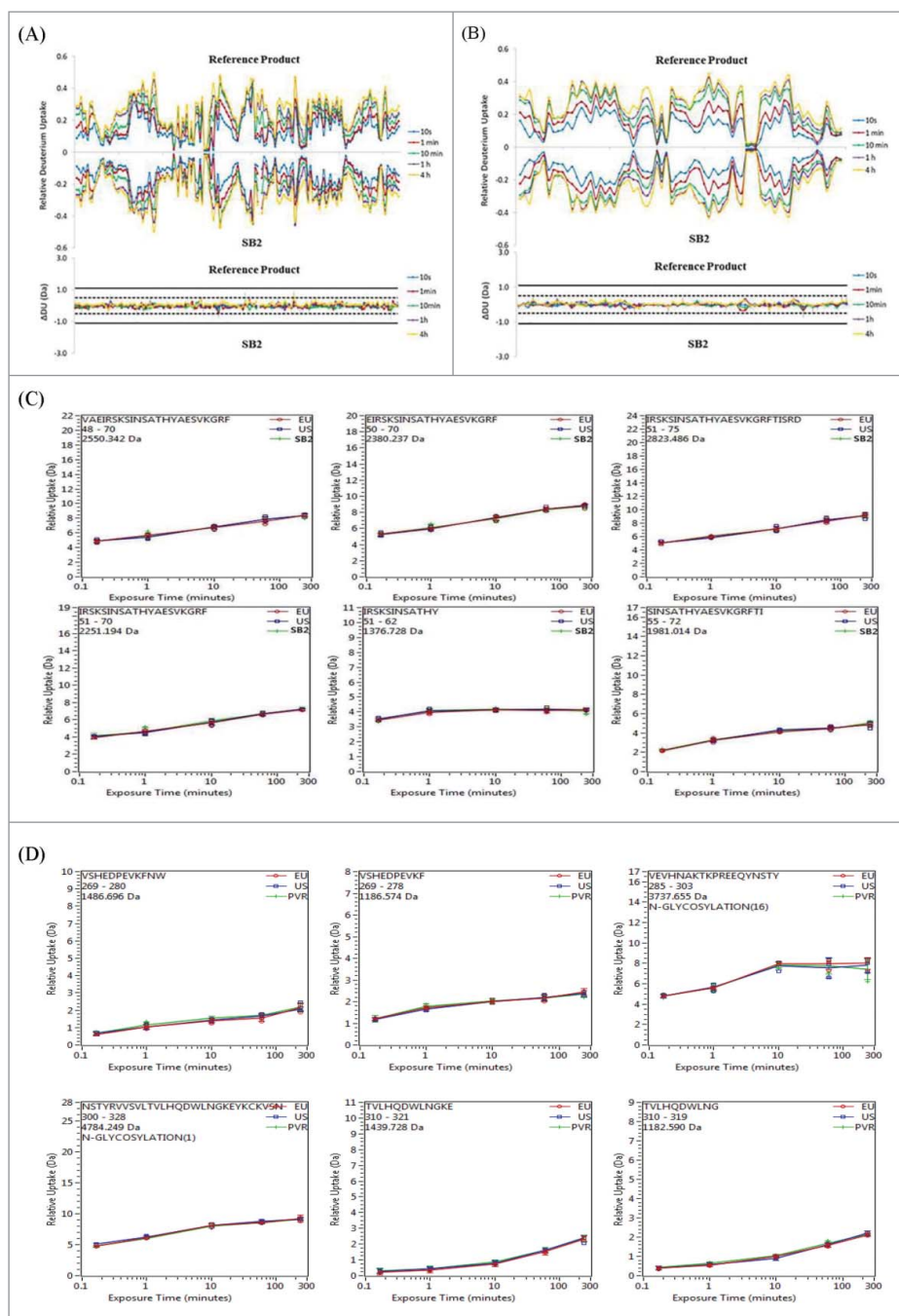


**Figure 5.** HDX Plots of SB2 and RP. (A) Butterfly plot for the heavy chain. (B) Butterfly plot for the light chain. (C) Plot for each representative peptide.

than 50%; this difference suggests that there is a less than 0.1% difference in epitope exposure between SB2 and RP.<sup>22</sup> These results confirmed the HDX/MS result that indicated the conformation of SB2 was similar to that of RP.

### Aggregation

In biologic products, aggregation, along with the size heterogeneity of aggregates, are known to enhance immunogenicity and affect efficacy.<sup>23,24</sup> However, there are limitations in the ability of analytical technologies to detect aggregation of biotherapeutic proteins such as antibodies because of their large size and structural complexity.<sup>25</sup> In accordance,

comprehensive comparability exercises were conducted with state-of-the-art and orthogonal analytical technologies of sedimentation velocity analytical ultracentrifugation (SV-AUC), size exclusion chromatography coupled to multi-angle laser light scattering (SEC/MALLS), dynamic light scattering, and size-exclusion chromatography coupled to UV detector (SEC/UV). The relative content of high-molecular-weight aggregates (%HMW) identified by the SEC/UV method was slightly higher for SB2 than for RP (Fig. 7A). However, the difference in %HMW was considered to be at trace levels when it was compared with the relative content of monomer (%monomer), which was more than 99% for both products. In addition, aggregate heterogeneity analyzed



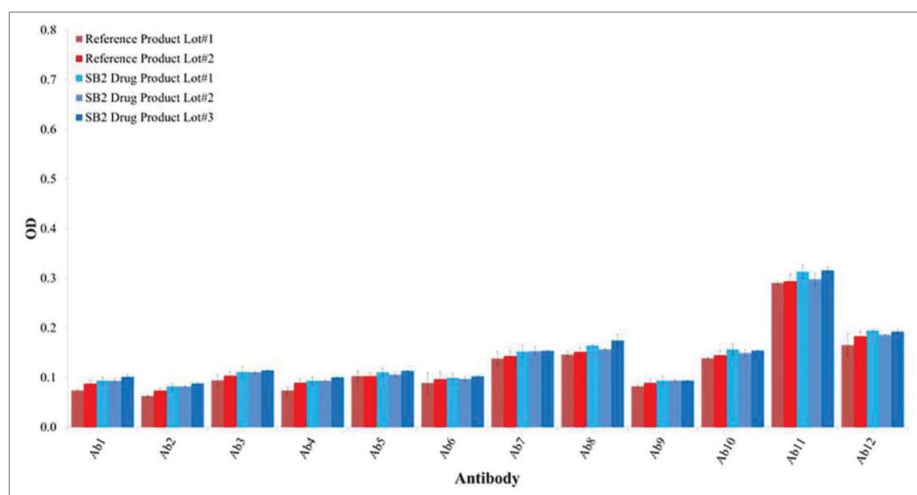


**Figure 6.** Antibody Conformational Array Results of SB2 and RP (Variable Region).

by SEC/MALLS was shown to be comparable between SB2 and RP. The calculated mass of the SB2 HMW peak was  $332800 \pm 85400$  Da and RP HMW peak was  $334800 \pm 97880$  Da. Both values correspond to the dimeric form (data not shown).

In addition, SV-AUC was employed as a powerful orthogonal method to SEC/UV because the samples are not exposed to extraneous conditions such as solid or mobile phases.<sup>25</sup> SV-AUC results showed that the size distribution of SB2 and RP was similar; namely the monomer, reversible dimer, and irreversible aggregates (Fig. 7B). Thus, similarity in the relative content of monomer, reversible dimer, and irreversible aggregates was apparent (Table 3). SV-AUC was also used to

compare physical characteristics between homologous, soluble macromolecules by measuring the coefficient of sedimentation ( $S_m$ ), which takes into account shapes and sizes. The respective  $S_m$  values of the monomer and reversible dimer were also comparable between SB2 and RP (Table 3).

### Fragmentation

Like aggregation, fragmentation is an important quality attribute related to safety and potency. SEC resulted in poor resolution between the monomer and low-molecular-weight (LMW) fragments; therefore, this method did not provide accurate quantitation of LMW impurities. Instead, capillary

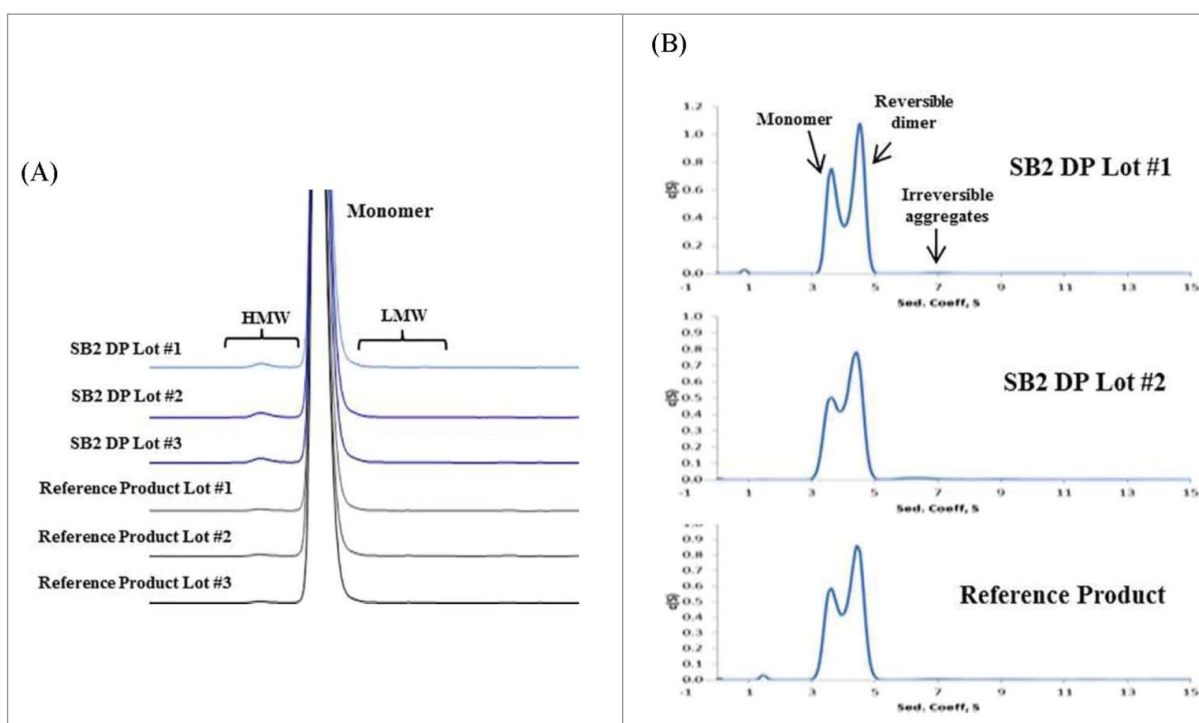


**Figure 7.** Size Exclusion Chromatographic Profiles and Sedimentation Coefficient Profiles of SB2 and RP. (A) Size exclusion chromatograms of SB2 and RP. (B) Sedimentation coefficient distribution plot.

**Table 3.** SV-AUC results for SB2 and RP.

Sample	Sedimentation Coefficient, S <sup>a</sup>			Fractions of Total, %			
	Weight-Averaged	Monomer	Reversible dimer	LMW	Monomer	Reversible dimer	Irreversible aggregates
SB2 DP Lot #1	4.099	3.696	4.453	0.7	43	57	0.0
SB2 DP Lot #2	4.020	3.672	4.382	0.0	43	56	1.3
RP(EU)	3.990	3.640	4.350	0.0	39	59	1.9
RP(US)	4.025	3.669	4.400	0.9	41	57	0.8

<sup>a</sup>S, Svedberg, a measure of the sedimentation coefficient:  $s. 1 S = 1013$  seconds.

electrophoresis-sodium dodecyl sulfate analysis (CE-SDS) was used to evaluate purity and LMW impurities in SB2 and RP. The results showed that the electrophoretic profiles of SB2 and RP were similar (Fig. 8), and the purity and the levels of LMW impurities in SB2 were similar to those of RP (data not shown). Therefore, SB2 and RP are considered similar in terms of fragmentation.

### Glycosylation

Glycosylation is a significant determinant of protein function, efficacy, clearance, and immunogenicity.<sup>26</sup> Infliximab is glycosylated with N-glycosylation structures linked to Asn<sub>300</sub> in the Fc region (Fig. 1). It has been reported that glycosylation of the Fc region is heterogeneous because of the presence of different terminal sugars, which may influence the binding of immunoglobulin G (IgG) to Fc receptors and C1q, and thus may affect Fc effector functions by changing the protein structure.<sup>27,28</sup> To elucidate the carbohydrate structure of SB2 and RP, we implemented state-of-the-art methods such as LC-ESI-MS/MS analysis alone (for the identification of N-glycosylation sites) and in combination with procainamide labeling (for the identification for N-glycan species), and 2-aminobenzamide (2-AB) labeling and hydrophilic interaction ultra-performance liquid chromatography (HILIC-UPLC) analysis (for characterization of the glycosylation profile).

LC-ESI-MS/MS analysis results showed that the N-glycosylation sites of SB2 and RP were identical and consistent with the theoretical site, Asn<sub>300</sub>, in the Fc region (data not shown). The N-glycan identification results analyzed by procainamide labeling and LC-ESI-MS/MS, and 2-AB labeling and HILIC-UPLC showed that the predominant forms were fucosylated bi-

antennary structures containing 0, 1, or 2 terminal galactose residues (i.e., G0F, G1F, and G2F) and an afucosylated bi-antennary structure with no terminal galactose (i.e., G0) in SB2 and RP. Most of the glycan species identified by LC-ESI-MS/MS were detected in 2-AB labeling and HILIC-UPLC analysis (Fig. 9A). However, a minor difference was observed in the N-glycan species between SB2 and RP. N-acetylneuraminic acid (NANA) was observed specifically in SB2, whereas N-glycolylneuraminic acid (NGNA) and galactose- $\alpha$ -1,3 galactose ( $\alpha$ -Gal) were observed in RP only. This difference could be attributed to different production cell lines; SB2 was manufactured using CHO cell lines instead of the murine cell lines (SP2/0) used for the production of Remicade<sup>®</sup>. It is well known that the major glycoforms of recombinant mAbs expressed in CHO, murine NS0, and murine SP2/0 cell lines are G0F, G1F, and G2F, but the major differences between CHO cell lines and the two murine cell lines are the presence of terminal N-glycolylneuraminic acid (NGNA) and galactose- $\alpha$ -1,3-galactose ( $\alpha$ -Gal) in recombinant mAbs expressed using murine cell lines.<sup>29</sup>

Although it is well known that NGNA and  $\alpha$ -Gal glycoforms are glycans that are not found in humans and therefore may elicit an unwanted immune response,<sup>30</sup> NGNA and  $\alpha$ -Gal represented minor isoforms in terms of quantity in RP, which did not affect the clinical outcomes. Additionally, new glycan species (e.g., NANA) were observed in SB2, but these glycan species are known to be common in humans and in CHO cells,<sup>31</sup> and they were also so low in quantity as not to be detected by 2-AB labeling and HILIC-UPLC analysis (only detected by procainamide labeling and LC-ESI-MS/MS analysis). Therefore, some minor differences in glycan species were not considered to affect the immunogenicity profile of SB2 and RP.

We conducted 2-AB labeling and HILIC-UPLC analysis to evaluate the similarity between SB2 and RP in both the N-glycan profile and its quantity. We quantified N-glycan species that were categorized as afucosylated glycans and mannosylchitobiose core without L-fucose (Total Afucose), neutral galactosylated glycans (Gal), and sialylated glycans (Charged) according to the terminal sugar, which may affect Fc effector functions, respectively. It is well known that not only afucosylated glycans but also high mannose glycans can affect Fc $\gamma$ RIIIa binding and ADCC activities;<sup>26</sup> therefore, it was not surprising that regression analysis showed that total afucosylated glycans in SB2 and RP was strongly correlated with Fc $\gamma$ RIIIa binding and ADCC activity.

The 2-AB labeling and HILIC-UPLC analysis found that the total Afucose content of SB2 was highly similar to RP (Fig. 9B). These findings are consistent with the Fc $\gamma$ RIIIa binding and

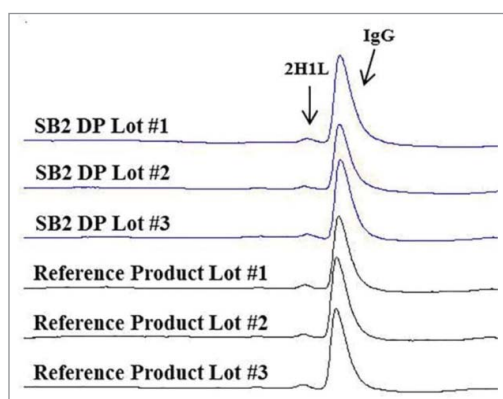


**Figure 8.** Non-reduced CE-SDS electropherograms of SB2 and RP.

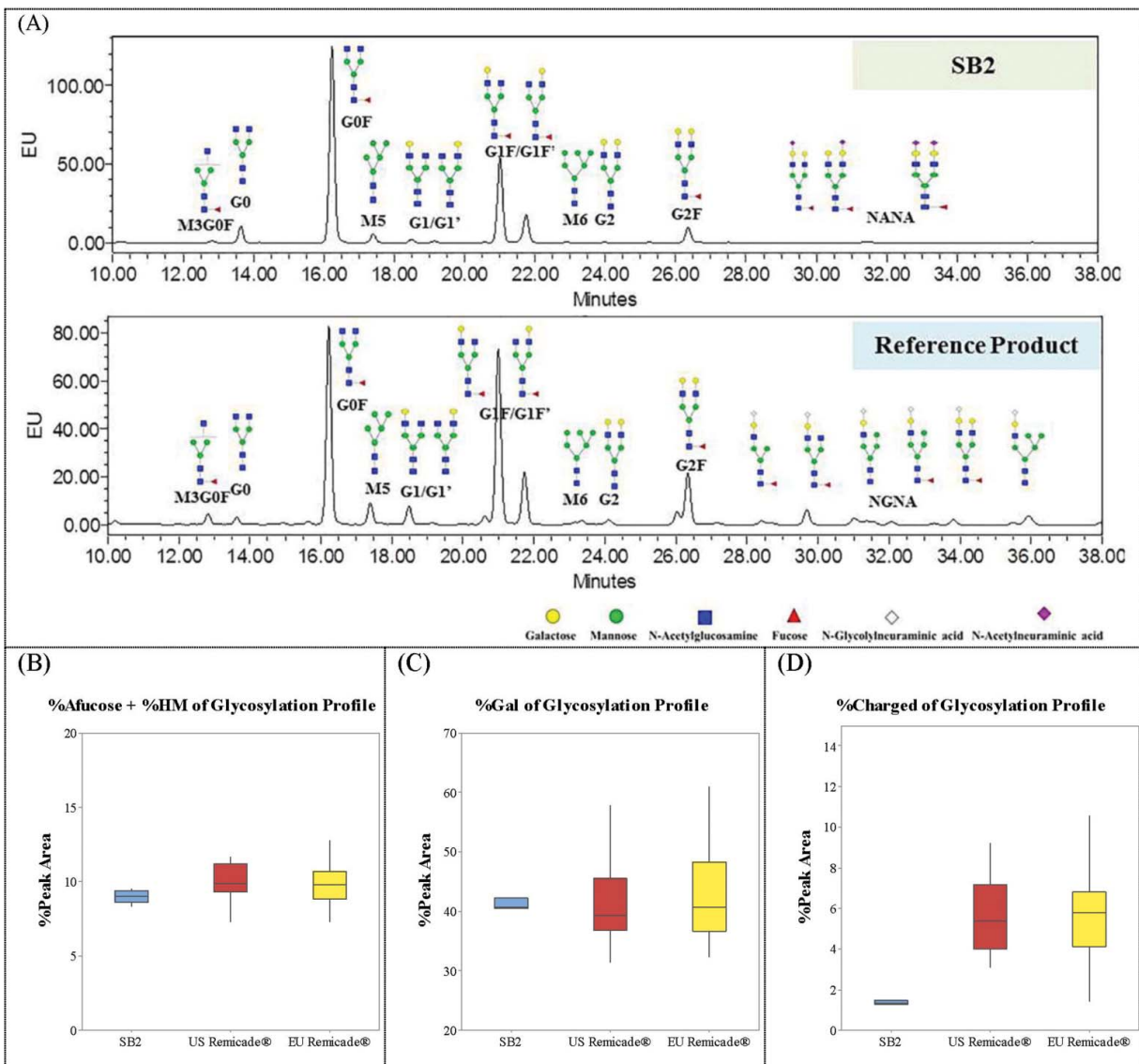


**Figure 9.** Glycosylation Profile of SB2 and RP. (A) Glycosylation profile. (B) %Total Afucosylated glycan. (C) %Galactosylated glycan. (D) %Charged glycan. (Red dot line: similarity range).

ADCC results (Fig. 14A and Fig. 14B). The Gal content of SB2 was also highly similar (Fig. 9C), but the charged content was slightly lower than that of RP (Fig. 9D). Antibodies with terminal sialic acids in Fc-glycosylation may cause a negative impact on ADCC, because of either reduced Fc $\gamma$ RIIIa binding on natural killer cells.<sup>32</sup> Furthermore, Fc sialylation with  $\alpha$ 2,6-linked sialic acid residues has been suggested to enable IgG to bind the C-type lectin DC-SIGN, thereby engaging a complex, Fc $\gamma$ RIIB-mediated anti-inflammatory mechanism potentially implicated in human intravenous immunoglobulin.<sup>33</sup> Accordingly, the SAR study and comparative assays using SB2 and RP were performed to rule out the uncertainty associated with the marginal difference of charged glycans on the products that could have an effect on the efficacy and safety of infliximab. The SAR study results showed that there was no significant difference in FcRn binding, Fc $\gamma$ RIIIa binding, and ADCC activities between sialylated and non-sialylated forms of both SB2 and RP, which were prepared by sialidase treatment. Hence, the slightly lower charged glycan content of SB2 is not considered to have a meaningful impact on efficacy of infliximab, based on SAR

study results as well as similar Fc $\gamma$ R binding activities including Fc $\gamma$ RIIB-binding activity.

### Charge heterogeneities

Charge heterogeneities may result from multiple causes such as deamidation, oxidation, and variations in C-terminal Lys, formation of N-terminal pyroglutamate, aggregation, isomerization, charged (sialylated) glycans, antibody fragmentation, glycation at Lys residues, and succinimide formation.<sup>34</sup> Charge profiles of SB2 and RP were assessed by CEX-HPLC analysis with CPB treatment and the results indicated that SB2 and the RP were similar (Fig. 10 and Fig. 11), whereas icIEF and CEX-HPLC analysis results without CPB treatment showed that basic variants of RP were much higher than that of SB2 (Fig. 11). To justify the different levels of basic variants between SB2 and the RP, and to gain further insights into the effect of charge variants on biological activity, we conducted a SAR study using SB2 and the RP.

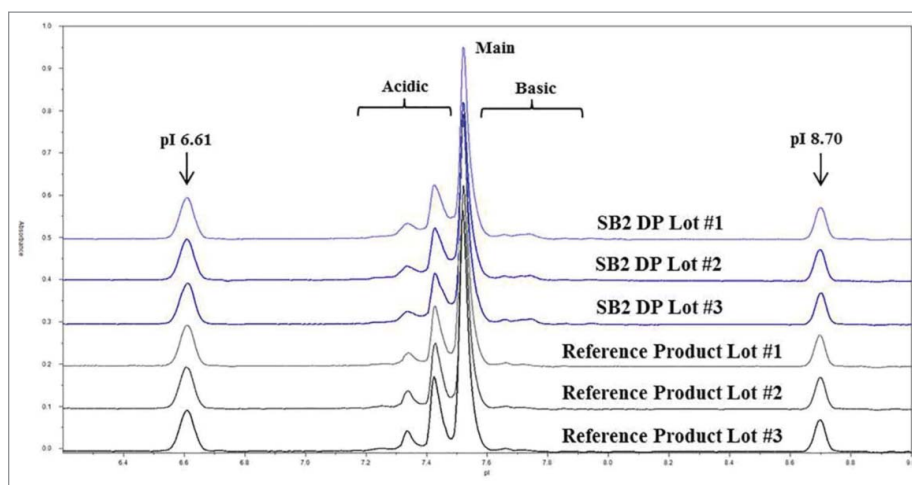


**Figure 10.** Charge Profiles of SB2 and RP by icIEF Analysis with CPB treatment. Comparison of SB2 (blue line) and RP (black line) for carboxypeptidase B-treated imaging capillary isoelectric focusing profiles. *pI* isoelectric point.

Major charge variants of SB2 and the RP were resolved and fractionated by CEX-HPLC (Fig. 12A), and each fractionated peak was analyzed by CEX-HPLC, peptide mapping by LC-ESI-MS/MS, biological assays such as TNF- $\alpha$  binding assays and Fc $\gamma$ RIIIa binding assays. Peptide mapping results showed that the observed difference in the acidic species of SB2 and RP was due to the presence of N-glycans rather than sialic acid (i.e., NGNA) at Asn<sub>300</sub> in RP, and these results were consistent with the glycosylation results. The difference in the basic species of SB2 and the RP was mostly due to the unprocessed Lys residue and  $\alpha$ -amidation at the C-terminus of the heavy chain (Fig. 12A). In samples not treated with CPB, unprocessed Lys variants were observed abundantly in RP and the  $\alpha$ -amidation

of the heavy chain at the C-terminal proline site was detected in SB2. Bioassays (TNF- $\alpha$  binding and Fc $\gamma$ RIIIa binding activities) were performed with each peak fractions, respectively, to gain further insights into the effect on the biological activity of infliximab. The results showed that there were no significant differences in TNF- $\alpha$  binding and Fc $\gamma$ RIIIa binding activities between SB2 and RP (Fig. 12B and Fig. 12C). These findings showed that the difference in basic variants between SB2 and RP was not considered to affect the biological activities of infliximab.

In an analysis of the difference in basic variants, Johnson et al.<sup>35</sup> confirmed that  $\alpha$ -amidation was common in recombinant monoclonal antibodies with a consensus sequence of -PGK at the C-terminus, and this modification had no effect on the antigen

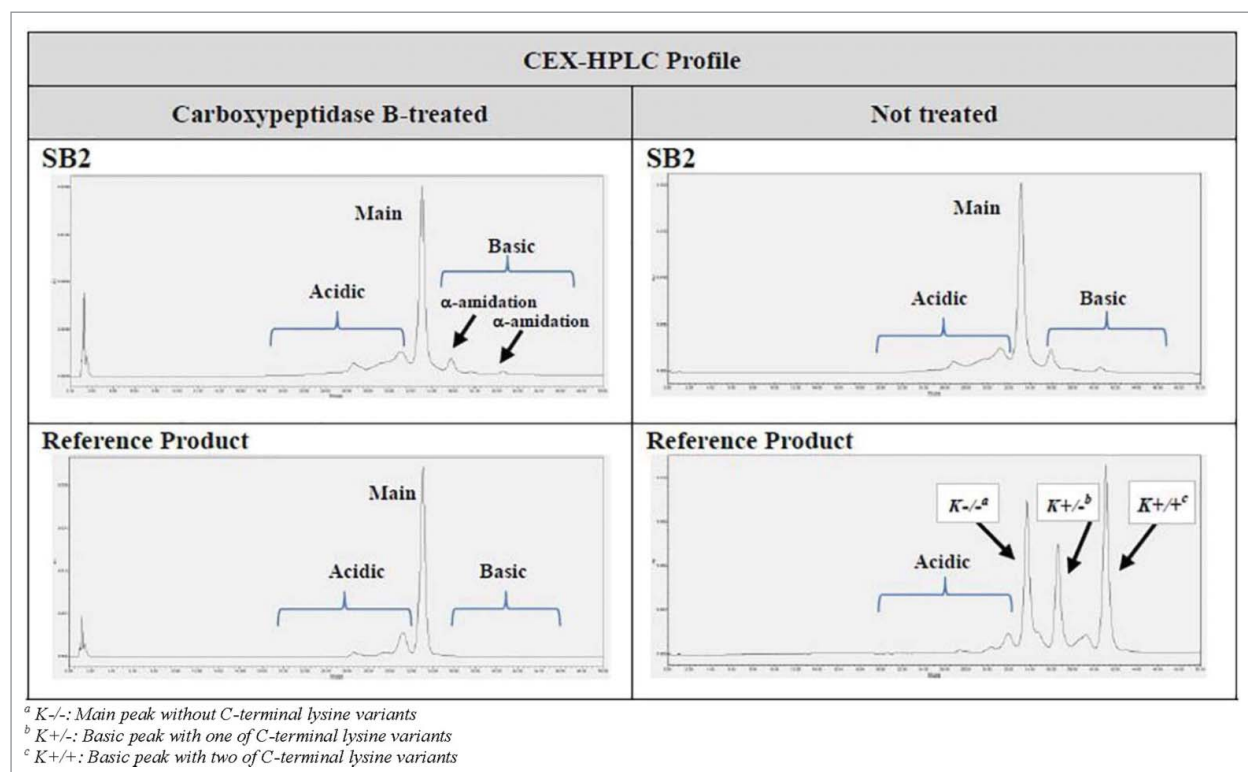


**Figure 11.** Charge Profiles of SB2 and RP by CEX-HPLC Analysis with CPB treatment (left-handed) and without CPB treatment (right-handed).

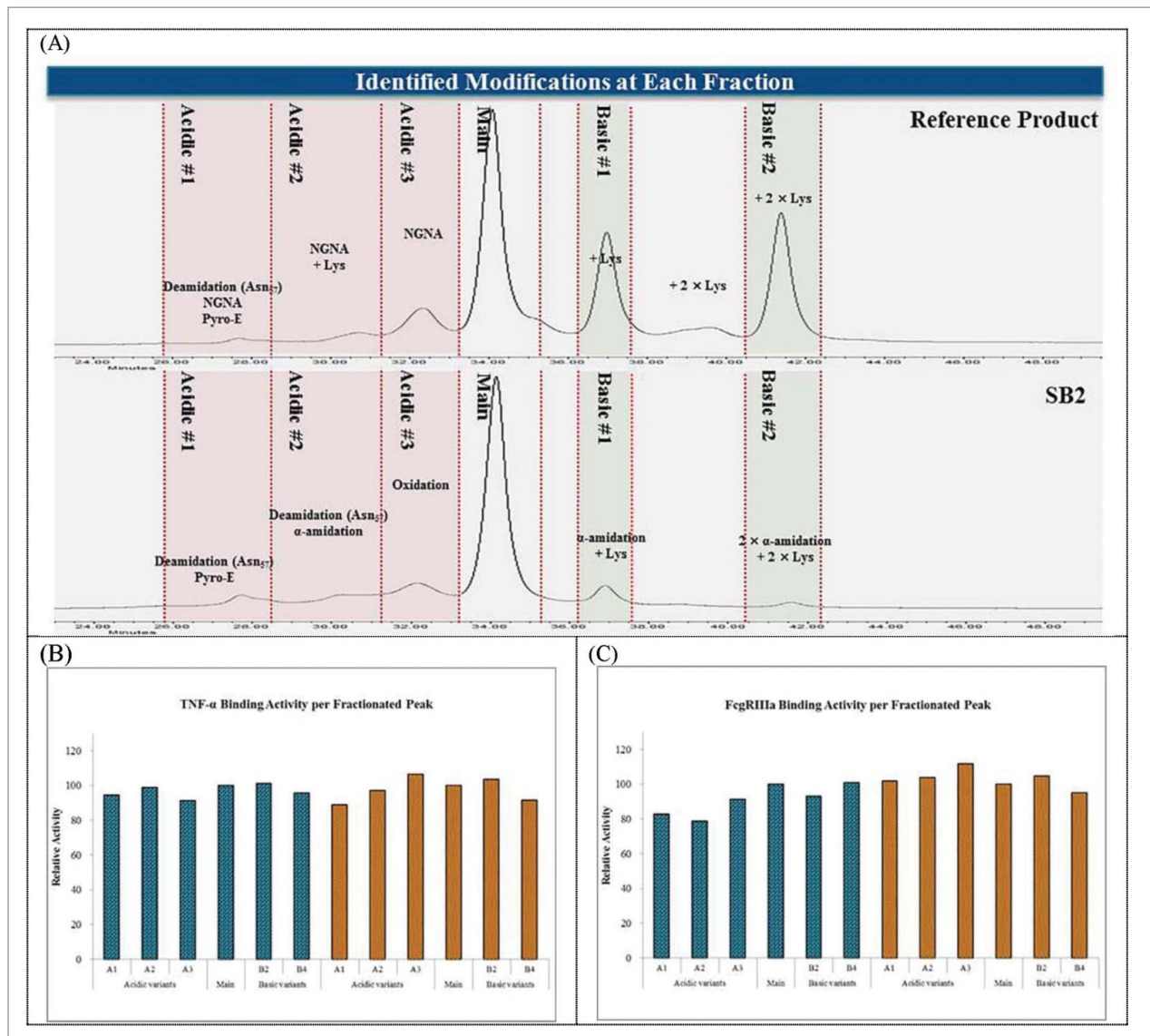


**Figure 12.** Structure and Activity Relationship Study Results on Charge Variants. (A) Modification identified at each CEX-HPLC fractionated peak of SB2 and RP without Carboxypeptidase B Treatment (B) TNF- $\alpha$  binding activity per fractionated peak (C) Fc $\gamma$ RIIIa binding activity per fractionated peak (NGNA; N-glycolylneuraminic acid, +Lys; containing C-terminal one Lys residue, Deamidation (Asn<sub>57</sub>); deamidation at Asn<sub>57</sub> in heavy chain,  $\alpha$ -amidation.;  $\alpha$ -amidation at proline carboxyl residue; pyro-E; pyroglutamic acid in N-terminus of heavy chain).

binding and Fc effector functions of the antibody. In addition, as  $\alpha$ -amidation has been commonly observed in biologically active peptides including peptide hormones and neurotransmitters in human, it is not considered an unnatural modification to the human immune system.<sup>36</sup> One common modification of therapeutic antibodies is the processing of C-terminal Lys (i.e., zero, one, or two C-terminal Lys residues) during the cell culture, yet this residue is generally absent from IgG found in serum due to clipping of the Lys residue.<sup>34</sup> Removal of C-terminal Lys has no effect on structure, thermal stability, antigen binding and potency, and FcRn binding and pharmacokinetics (PK) in rats.<sup>34</sup>

Therefore, these modifications were not considered to affect the efficacy and safety of infliximab.

### Fab-related biological activities

The main MOA of infliximab is the inhibition of TNF activity. Infliximab reduces inflammation by binding to TNF- $\alpha$ , thus

preventing it from binding to TNF receptors on the cell surface and inhibiting TNF receptor-mediated cell signaling.<sup>12</sup> TNF- $\alpha$  is known to exert unique biologic functions because it is a bipolar molecule that transmits signals both as a ligand and a receptor.<sup>37,38,39,40,41</sup> Based on this MOA, four biological assays were employed to evaluate the Fab-related biological quality of SB2: two TNF- $\alpha$  binding assays (one for soluble TNF- $\alpha$  [sTNF- $\alpha$ ] and another for transmembrane TNF- $\alpha$  [tmTNF- $\alpha$ ]), a TNF- $\alpha$  neutralization assay, and an apoptosis assay.

The relative sTNF- $\alpha$  binding activity of SB2 was similar to that of EU- and US-sourced RP. Mean percent relative binding activities were 97% for SB2, 99% for the EU-sourced RP, and 98% for the US-sourced RP. In addition, sTNF- $\alpha$  binding activity of all SB2 batches were similar to RP (Fig. 13A). Evaluation of the potency of SB2 by the TNF- $\alpha$  neutralization assay using the luciferase reporter gene showed the mean percent relative potencies were 96% for SB2, 100% for EU-sourced RP, and 101% for US-sourced RP. All SB2 batches were also similar to

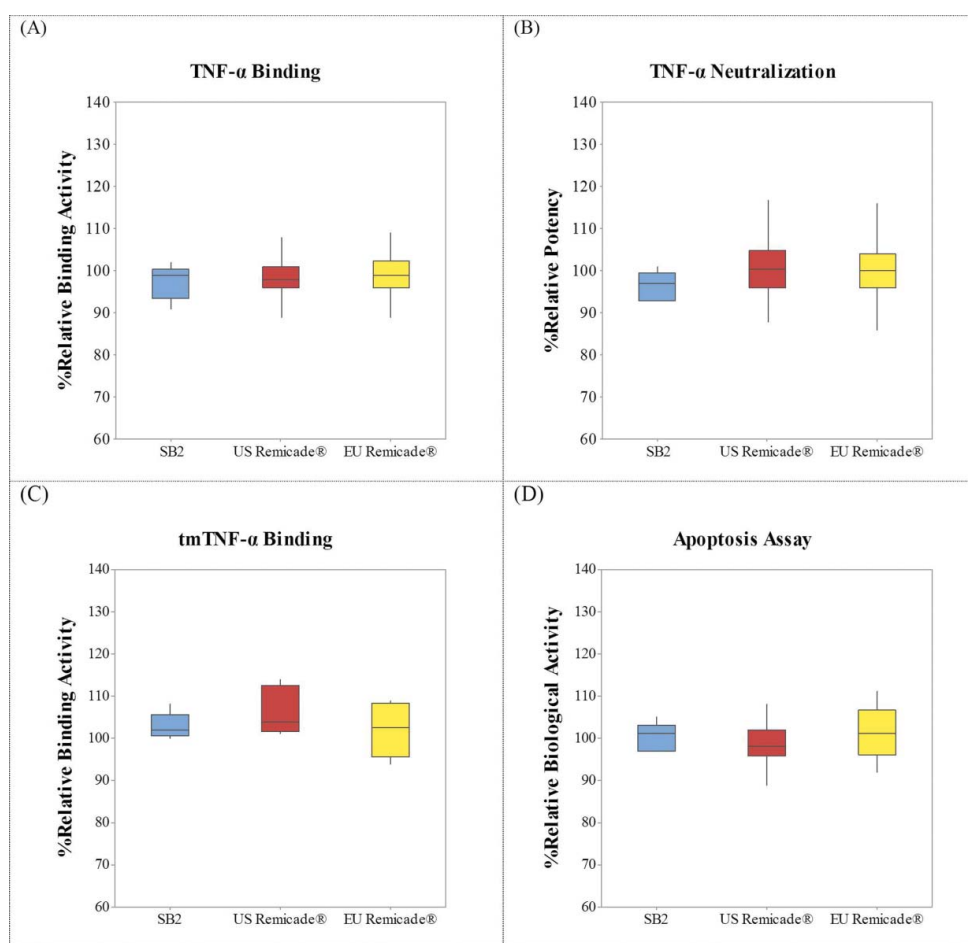


**Figure 13.** Comparison of the Fab-related Biological Activities of SB2 and RP. (A) TNF- $\alpha$  binding activity. (B) TNF- $\alpha$  neutralization activity. (C) tmTNF- $\alpha$  binding affinity. (D) Apoptosis activity. Side-by-side comparison was made for tmTNF- $\alpha$  binding affinity. (Legend: (a) confidence interval of mean difference between SB2 and US Remicade<sup>®</sup>. (b) confidence interval of mean difference between SB2 and EU Remicade<sup>®</sup>. (c) confidence interval of mean difference between US and EU Remicade<sup>®</sup>. Red dot line: similarity range).

RP (Fig. 13B). In case of reverse signaling, there was no statistically significant difference between the tmTNF- $\alpha$  binding activity of SB2 and that of EU-sourced and US-sourced RP (Fig. 13C). SB2 also exhibited apoptosis activity similar to that of the EU-sourced and US-sourced RP in a Jurkat-mTNF- $\alpha$  cell system (Fig. 13D).

### Fc-related biological activities

The Fc region of infliximab binds to two distinct classes of Fc receptors: a family of Fc $\gamma$  receptors (Fc $\gamma$ R) found primarily on leukocytes and a family of neonatal Fc receptors (FcRn) for IgG expressed primarily on endothelial cells.<sup>42</sup> Fc $\gamma$ Rs contribute to immune response modulation by activation or inhibition of cellular signal transduction related to inflammatory reactions or stimulation of immune effector cells. Among several Fc $\gamma$ Rs, Fc $\gamma$ RIIIa is involved in ADCC. FcRn plays an important role in determining the half-life of serum IgG. In addition to Fc $\gamma$ RIIIa and FcRn, other components of the immune system such as complement also interact with the Fc portion of infliximab. Complement C1q binds to antigen-antibody immune complexes via the Fc region and mediates CDC.

Fc $\gamma$ RIIIa binding affinity was evaluated by surface plasmon resonance (SPR). Mean Fc $\gamma$ RIIIa binding affinities of SB2, EU-

sourced RP, and US-sourced RP were  $1.29 \times 10^{-6}$  M,  $1.14 \times 10^{-6}$  M, and  $1.17 \times 10^{-6}$  M, respectively. Binding affinities of all SB2 batches were within the predetermined similarity range (Fig. 14A). ADCC activity, which is closely related to Fc $\gamma$ RIIIa, was measured by using peripheral blood mononuclear cells (PBMCs) as effector cells. Mean percent relative ADCC activities of SB2, EU-sourced RP, and US-sourced RP were 122%, 118%, and 127%, respectively, against a reference standard, (Fig. 14B). SB2 also showed FcRn binding activity, which could affect PK profile, within the predetermined similarity range (Fig. 14C). C1q binding activity and CDC activity of SB2 were similar to those of RP (Fig. 14D, Fig. 14E). Binding activities to other Fc $\gamma$ Rs such as Fc $\gamma$ RIa, Fc $\gamma$ RIIa, Fc $\gamma$ RIIb, and Fc $\gamma$ RIIIb, were also similar.

### Discussion

EMA and US FDA guidelines for demonstrating the comparability of a biosimilar to a RP require more sophisticated methods and comprehensive characterizations than those used to assess batch-to-batch comparability of a biologic product that has undergone a manufacturing change.<sup>14,15,18</sup> Therefore, we evaluated more than 80 lots of RP to establish similarity ranges for use in monitoring quality shifts over time and for

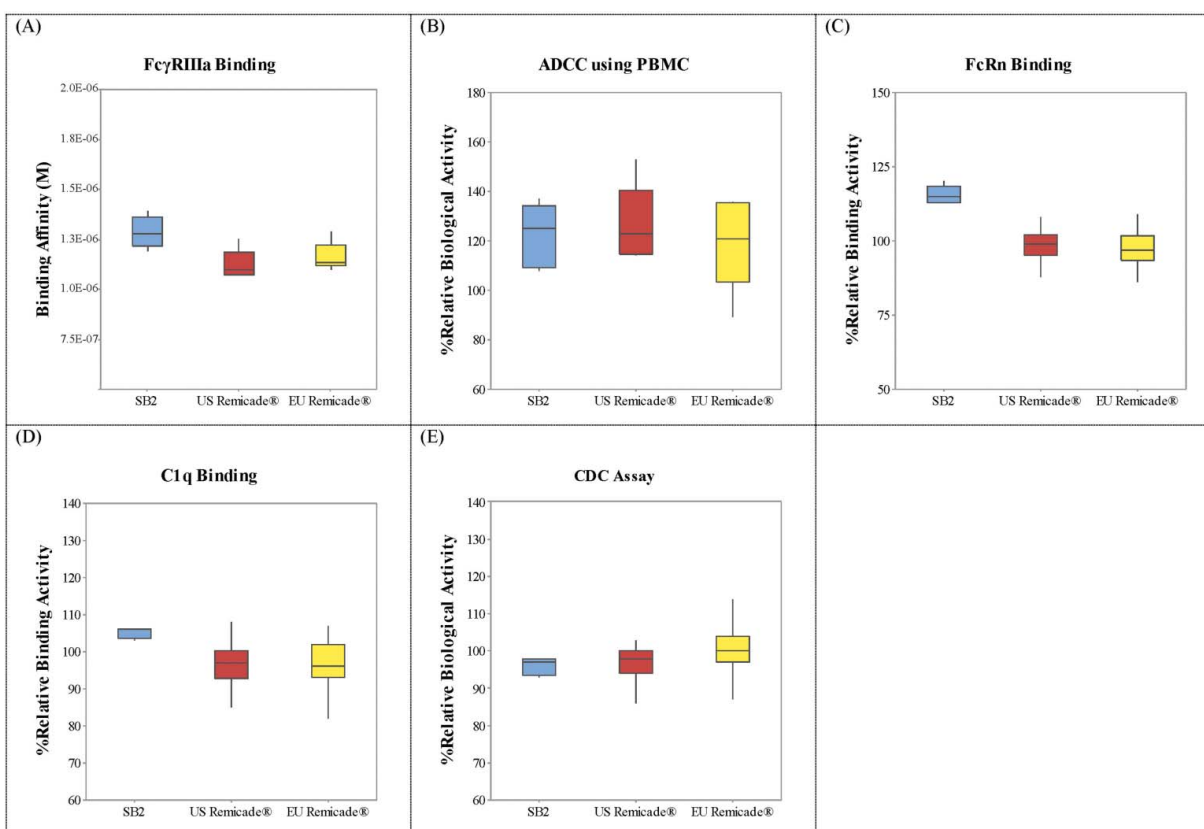


**Figure 14.** Comparison of the Fc-related Biological Activities of SB2 and RP. (A) Fc $\gamma$ RIIIa binding affinity by SPR. (B) ADCC using healthy donor PBMCs. (C) FcRn binding activity by AlphaScreen<sup>®</sup>. (D) C1q binding activity by ELISA. (E) CDC activity. Side-by-side comparison was made for Fc $\gamma$ RIIIa binding affinity and ADCC activity using healthy donor PBMCs. (Red dot line: similarity range).

comparability exercises between SB2 and RP. In total, more than 120 lots of RP from different market sources (e.g., EU, US, Canada, Australia, Japan, Switzerland, and Korea) with different expiry dates were purchased and tested in parallel with the establishment of biosimilarity. We used more than 60 state-of-the-art methods to analyze structural, physicochemical, and biological characteristics, and a subset of the results are summarized in Table 1.

Similarity ranges and side-by-side comparative approaches were used to demonstrate the analytical similarity of SB2 to RP in accordance with the regulatory requirements. Overall, physicochemical and biological characteristics of SB2 and RP were determined to be similar, but there were a few differences observed in physicochemical attributes between SB2 and the RP, which could be attributed to the difference in expression system; SB2 was manufactured using CHO cell lines, while Remicade<sup>®</sup> was manufactured using murine cell lines (SP2/0). As mentioned above, the supportive evidence from the literature and the results of SAR studies demonstrated that they were unlikely to affect the efficacy and safety of infliximab.

Although recombinant antibodies are generally considered to be well tolerated and non-toxic, repeated administration may induce immunogenicity. In accordance, a slight difference observed in physicochemical attributes was thoroughly evaluated to predict their lack of impact on the immunogenicity of SB2.

Charge variants or glycosylation profile may directly or indirectly influence protein immunogenicity by inducing conformational changes that lead to new epitopes or the shielding of

immunogenic epitopes.<sup>43,44</sup> To further evaluate the conformational similarity between SB2 and RP, an antibody conformational assay (enzyme-linked immunosorbent assay [ELISA]) was performed with SB2 and the RP in a side-by-side manner, together with HDX/MS analysis. The results suggested that new epitope exposure was not observed in either SB2 or the RP (Fig. 5 and Fig. 6). Therefore, the differences in charged glycans and charge variants between SB2 and RP were unlikely to affect the immunogenicity of SB2. According to the SEC analysis, the relative content of HMW species in SB2 was slightly greater than that in the RP, the heterogeneity of HMW aggregates analyzed by SEC/MALLS and SV-AUC were comparable between SB2 and RP, and the relative amount of HMW species was very low (less than 1%). Therefore, we believe that they are not likely to have an effect on SB2 immunogenicity, which was supported by the clinical outcome.

In addition, for further investigation on the correlation between the level of HMW aggregate and immunogenicity, we researched any potential association from the scientific literature and the public results for Remsima<sup>™</sup>, an infliximab biosimilar that is marketed in Europe and other regions. The relationship between the relative content of HMW species detected by the in-house SEC method and the incidence of anti-drug antibodies (ADAs) reported from clinical trials of Remsima<sup>™4</sup> was evaluated. From analyses using the SEC method, HMW level of the infliximab biosimilar was higher than that of RP. However, in the clinical trials of the infliximab biosimilar, the ADA incidence was comparable to that of the

RP.<sup>4</sup> In summary, the predictions based on quality findings were confirmed by clinical results demonstrating that the observed differences in HMW aggregates do not affect immunogenicity. In addition, there was no scientific evidence to support a causative association between such differences in HMW aggregates and ADA development in infliximab.

The results described herein are only part of the totality of evidence concerning the overall biosimilarity in terms of quality, efficacy, and safety, and these analytical similarity assessment results supported the conclusion that SB2 and RP are similar in terms of clinical efficacy and safety.

## Materials and methods

More than 80 lots of Remicade<sup>®</sup> (100 mg per vial; Johnson & Johnson), sourced from the EU and the US, were purchased and analyzed to establish the similarity ranges for CQAs and for a subgroup of non-CQAs throughout the development of SB2. Multiple lots of SB2 drug product and drug substance were also used. The similarity ranges for various quality attributes can be determined by appropriate statistical approaches. For this study, we used a two-tiered statistical tolerance approach (mean  $\pm$  kSD) and available data points to determine similarity ranges. Such an analysis yields a tolerance interval (with a k factor) that is within a specified confidence level and is guaranteed to have a particular proportion of the population. This tolerance interval is considered to be a probability interval. The analytical similarity assessment consists of general methods and a comprehensive battery of physicochemical and biological assays to address functionally important attributes. More than 60 structural, physicochemical, and biological assays were employed to analyze similarity between SB2 and the RP. A subset of the results is summarized in Table 1.

### Peptide mapping

The method of peptide mapping has been previously described.<sup>10</sup> Each sample (200  $\mu$ g) was mixed with 2  $\mu$ L of 1 M dithiothreitol and diluted with 8 M urea to achieve a final volume of 200  $\mu$ L. After 30 minutes of incubation at room temperature, 4  $\mu$ L of 1 M iodoacetamide were added, and each sample was incubated for 15 minutes at room temperature in the dark. Samples were then loaded onto a 10K molecular weight cut-off spin column. After three rounds of centrifugation, the buffer was replaced with 300  $\mu$ L of 50 mM Tris-HCl, pH 7.8, and the samples were digested initially with Lys-C (Roche, 11047825001) or trypsin (Roche, 11047841001) at 37°C for 16 hours.

After digestion with trypsin, the peptides underwent reverse-phase ultra-performance liquid chromatography (UPLC) MS using a BEH300 C18 column (Waters, 186003687/1.7  $\mu$ m, 2.1 mm  $\times$  150 mm) at 60°C. Elution of peptides was achieved by a linear gradient of 0–35% of mobile phase B (mobile phase A, 0.1% formic acid in water; mobile phase B, 0.1% formic acid in acetonitrile) at a flow rate of 0.3 mL/min for 100 minutes, and the peptides were analyzed by the Synapt-G2 system. Data were collected and processed by MassLynx (Waters) v4.1.

### Disulfide linkage mapping

The disulfide bonds of SB2 and RP were analyzed by LC-ESI-MS/MS. Samples were denatured with 8 M urea and digested with trypsin. After enzymatic digestion, peptides were analyzed chromatographically with MS detection. Disulfide-linked peptide peaks were detected under non-reducing conditions, and those peaks containing cysteine residues were detected after treatment with dithiothreitol for reduction of disulfide bonds. The mass of each disulfide-linked peptide was analyzed and manually assigned.

### Molecular weight analysis

The molecular weights of intact and deglycosylated SB2 and RP were determined by UPLC coupled to electrospray ionization mass spectrometry under non-reducing and reducing conditions, respectively. Ten micrograms of each sample was injected and data in the m/z range of 700–3000 amu were acquired. MassLynx software was used to deconvolute the MS spectra to produce molecular mass data. This software processes data on the basis of the maximum entropy algorithm.

### Circular dichroism

As an analytical method that measures the difference in left- and right-handed circularly polarized light, CD is divided into far-UV spectrum (190–250 nm) and near-UV spectrum (250–350 nm). Far-UV radiation is used to measure the secondary structure of proteins, whereas near-UV radiation is used to measure the tertiary structure of proteins.<sup>45</sup>

All samples were dialyzed in a solution of 10 mM NaPO<sub>4</sub>, 200 mM NaCl, pH 6.8, and 0.01% polysorbate 80. CD measurements were obtained with an AVIV 62 DS spectrophotometer with cells having a 0.5-cm path length for near-UV radiation and cells having a 0.1-cm path length for far-UV radiation.

### Intrinsic fluorescence analysis

ITF is an indirect method in which the shift in ITF intensities before and after denaturation are evaluated to determine the three-dimensional structure of a protein.<sup>46</sup>

Samples were dialyzed in a solution of 6.1 mM NaPO<sub>4</sub>, pH 7.2, 5% sucrose, and 0.05% polysorbate-80. For ITF assays under native conditions, the dialyzed samples were diluted with the same buffer to a concentration of 0.12 mg/mL and incubated at 4°C overnight before the spectra were obtained. For assays in denaturing conditions, the samples were diluted to a concentration of 0.12 mg/mL in a denaturing buffer (5 mM NaPO<sub>4</sub>, 5% sucrose, 0.01% polysorbate-80, 8 M guanidine HCl, pH 7.2) and incubated at 4°C overnight before the spectra were obtained.

### Differential scanning calorimetry

The method of DSC has been described previously.<sup>10</sup> Melting temperature T<sub>M</sub> of samples was analyzed by using a Thermal A MicroCal VP-Capillary (GE Healthcare). The sample and the corresponding buffer were heated at a rate of 60°C/h over



a range of 10°C to 95°C, and the  $\mu$ -DSC cell was pressurized to prevent boiling during heating. Prior to the run, samples were diluted to approximately 1.0 mg/mL in the placebo buffer. Baseline values were established by filling reference and sample cells with water and scanning them twice from 10°C to 95°C (heating rate of 60°C/h). Next, the sample was analyzed: the reference cell was filled with formulation buffer and the sample cell was filled with the formulation blank as well in order to subtract baseline values from each sample measurement. Thermal data were normalized on the basis of protein concentration. The  $T_m$  of the protein was determined from the heating scan data, which were analyzed by Origin 7.0 DSC software.

### Hydrogen/deuterium exchange

The method of HDX, which has been previously described,<sup>10</sup> was adapted to compare higher order structures. Samples were dialyzed in 25 mM  $\text{Na}_3\text{PO}_4$  and 100 mM NaCl, pH 6.3, and brought to a concentration of 2.5 mg/mL. The exchange was initiated by a 1:10 dilution of sample in  $\text{D}_2\text{O}$  at intervals of 10 seconds, 1 minute, 10 minutes, 1 hour, and 4 hours before quenching and injection onto the HDX sample manager (Waters). Peptides were digested on an immobilized pepsin column, and the fragments were eluted with a gradient of 5% to 95% acetonitrile over 15 minutes. Mass spectra were collected in  $\text{MS}^E$  mode, and peptide identification was accomplished by the ProteinLynx Global Server™ (PLGS, Waters). DynamX software (Waters) was used to calculate deuterium uptake and to generate butterfly and difference plots.

### Antibody conformational array

All antibodies and ELISA kits used in this study were commercial kits manufactured by Array Bridge Inc. (St. Louis, Missouri). For the sandwich ELISA, antibodies against each peptide covering the entire region of infliximab were coated on 96-well plates. In each column of the coated plates, SB2 and EU-sourced RP were incubated in triplicate. A biotin-labeled rabbit anti-human IgG antibody was used to detect the infliximab-anti-peptide antibody complex, and streptavidin-HRP was used to detect the complex formed by the three components (i.e., anti-human IgG– infliximab-anti-peptide antibody). The average of triplicate readings was used to calculate the difference.  $\Delta\text{OD}$  is equal to the difference between the mean OD value of the testing sample and the mean OD value of the reference material ( $\text{OD}_{\text{TS}} - \text{OD}_{\text{RM}}$ ), and the  $\text{OD}_d$  is calculated by dividing  $\Delta\text{OD}$  by the mean OD of the reference material ( $\text{OD}_d = \Delta\text{OD}/\text{OD}_{\text{RM}}$ ).<sup>43</sup>

### Size exclusion chromatography

HMW species of the proteins were measured by using a TSK G3000SWXL column (Tosoh, 008541, 5  $\mu\text{m}$  / 7.8 mm  $\times$  300 mm) at a flow rate of 1.0 mL/min with a mobile phase of 100 mM sodium phosphate and 500 mM L-arginine monohydrochloride, pH 6.8. Samples were injected and UV detection was performed at 280 nm. Data were acquired and processed by Empower™ 3 (Waters) software. Results are presented as the relative monomer content and HMW content.

### Sedimentation velocity-analytical ultracentrifugation

As an orthogonal method to SEC, SV-AUC was conducted to evaluate the comparability of protein aggregation profiles between samples, which were in 6.1 mM  $\text{Na}_3\text{PO}_4$ ; 5% sucrose; and 0.05% polysorbate-80, pH 7.2. Samples were analyzed by the Beckman XLA-70 analytical ultracentrifuge system with the acquisition parameters of 120,000 g, a temperature of 5°C, and UV wavelength detection at 280 nm. Two separate scans of each sample were performed. The SEDFIT parameters were used to process sample data.

### Capillary electrophoresis-sodium dodecyl sulfate

Our method of CE-SDS has been described previously.<sup>10</sup> CE-SDS analyses (reducing and non-reducing) were conducted with a high-performance capillary electrophoresis system (PA 800 plus Pharmaceutical Analysis System; Beckman). For the reducing condition, 400  $\mu\text{g}$  of sample was mixed with 2  $\mu\text{L}$  of a 10-kDa internal standard, 87  $\mu\text{L}$  of SDS-MW sample buffer (Beckman Coulter, A10663), and 5  $\mu\text{L}$  of 2-mercaptoethanol and heated at 70°C for 10 minutes. For the non-reducing condition, iodoacetamide replaced 2-mercaptoethanol, and the sample was electrokinetically introduced onto a capillary (Beckman Coulter, bare fused-silica capillary, 50  $\mu\text{m}/30.2$  cm) and was separated in the capillary cartridge. Electrophoresis was performed at a constant voltage (applied field strength, -497 V), and progress was monitored by UV detection (wavelength, 220 nm) through the capillary window and aperture (Beckman Coulter, 144712, 100  $\times$  200  $\mu\text{m}$ ). Acquired data were processed by 32 Karat software with integration capabilities.

### Imaged capillary isoelectric focusing

Charge heterogeneities were measured by icIEF and CEX. A total of 100  $\mu\text{g}$  of sample was treated with CPB for 2 hours to remove the unprocessed Lys residue at the C terminus of the heavy chain. Each 60  $\mu\text{g}$  of CPB-treated sample was mixed with 8  $\mu\text{L}$  of Pharmalyte 3–10, 70  $\mu\text{L}$  of 1% methyl cellulose, 25  $\mu\text{L}$  of 8 M urea, 83.5  $\mu\text{L}$  of distilled water, 1  $\mu\text{L}$  of pI 6.61 marker, and 0.5  $\mu\text{L}$  of pI 8.70 marker. A sample of 160  $\mu\text{L}$  of the total mixture was loaded onto an ICE3 icIEF instrument by using a capillary cartridge at 4°C. The anolyte and catholyte were 0.08 M  $\text{H}_3\text{PO}_4$  and 0.1 M NaOH, respectively.

### Cation exchange chromatography

CEX analysis was used as an orthogonal method to icIEF for the assessment of charge variants. CEX analysis was performed with a MAbPac SCX-10 (ThermoScientific, 4.0 mm  $\times$  250 mm) connected to a Waters HPLC/UV system. A 20  $\mu\text{g}$  sample was digested by CPB and then injected. UV detection was performed at a wavelength of 280 nm. Results were reported as relative percent charge variants (e.g., % of acidic variants, % of main peak, and % of basic variants).

### **Glycosylation profile by 2-AB labeling and HILIC-UPLC analysis**

For quantitative determinations, 100  $\mu\text{g}$  of sample was denatured in sodium dodecyl sulfate and dithiothreitol, and treated with PNGase F for about 18 hours to release N-glycans. They were precipitated in cold ethanol, and the precipitate was dried. The precipitated N-glycans were then labeled with 2-AB for 3 hours. Samples were injected onto a UPLC BEH glycan column (2.1 mm  $\times$  150 mm, 1.7  $\mu\text{m}$ ). The labeled N-glycans were separated at a flow rate of 0.5 mL/min with mobile phase A (50 mM ammonium formate) and mobile phase B (100% acetonitrile). The signal was detected by a fluorescence detector at an excitation wavelength of 330 nm and an emission wavelength of 420 nm.

### **TNF- $\alpha$ binding assay**

TNF- $\alpha$  binding activity of SB2 was measured by a competitive inhibition binding assay using time-resolved fluorescence resonance energy transfer (TR-FRET). In this assay, Europium chelate-labeled infliximab competes with unlabeled sample for binding to Cy5-labeled TNF- $\alpha$ . Fixed concentrations and volumes of Europium chelate-labeled material and Cy5-labeled material were added to the assay plate containing the sample. The plate was incubated for 1 hour at ambient temperature with moderate agitation. The fluorescence signal, which is inversely proportional to TNF- $\alpha$  binding activity, was measured at a wavelength of 665 nm on a microplate reader (Envision<sup>®</sup> multilabel reader, PerkinElmer).

### **TNF- $\alpha$ neutralization assay**

The inhibitory activity of SB2 on the TNF- $\alpha$  signaling pathway was measured by a TNF- $\alpha$  neutralization assay that uses a luciferase reporter gene cell line that contains an NF- $\kappa\text{B}$  binding sequence upstream of the luciferase reporter gene. The binding of TNF- $\alpha$  to the cell surface TNF receptor leads to a signal cascade activating NF- $\kappa\text{B}$ , which then activates expression of the luciferase reporter gene. By measuring luciferase activity, the inhibitory effect of infliximab can be assessed. TNF- $\alpha$  was mixed with each sample, and they were incubated at room temperature for 20 to 40 minutes in a 96-well assay plate. After incubation, cells were transferred to wells in the assay plate and incubated for 24 hours. Luciferase activity was measured by using Steady-Glo<sup>®</sup> Luciferase Assay System (Promega).

### **Apoptosis assay**

The effect of SB2 on apoptosis activity was determined by measuring caspase activity in Jurkat cells that expressed membrane TNF- $\alpha$ . Jurkat-mTNF- $\alpha$  cells were incubated with SB2 for 24 hours at 37°C in an atmosphere of 5% CO<sub>2</sub>. After incubation, Caspase-Glo<sup>®</sup> was added and the luminescence signal was induced by cleavage of the pro-luminogenic peptide substrate. The luminescence signal, which was proportional to apoptosis activity, was measured by a luminometer.

### **tmTNF- $\alpha$ binding assay**

The tmTNF- $\alpha$  binding activity of SB2 was determined by flow cytometry. Jurkat-mTNF- $\alpha$  cells were incubated with sample to which PE-labeled secondary antibody was added. Fluorescence-activated cell sorting was used to measure fluorescence intensity, which indicated the binding activity of SB2 to TNF- $\alpha$  on the surface of Jurkat-mTNF- $\alpha$  cells.

### **FcRn binding assay**

FcRn binding activity was evaluated in an amplified luminescence proximity homogeneous assay (AlphaScreen<sup>®</sup>, PerkinElmer). Two signaling beads were used: hydrogel-coated donor beads and acceptor beads that provided functional groups for conjugation to biomolecules. The donor beads were coated with streptavidin, whereas the acceptor beads were coated with a human IgG1 antibody. FcRn-Fc was tagged with biotin. All three components were mixed with sample in an assay plate, and the plate was incubated at ambient temperature with mild agitation. Luminescence signals were measured by a microplate reader. Laser excitation (wavelength, 680 nm) of a photosensitizer present on the donor bead results in the conversion of ambient oxygen to a more excited singlet state. The singlet-state oxygen molecules diffuse to react with a thioxene derivative on the acceptor bead, which results in generation of chemiluminescence at 370 nm. It further activates fluorophores contained on the same bead, and the fluorophores subsequently emit light at wavelengths of 520–620 nm. Measured signal was inversely proportional to FcRn binding activity of the sample.

### **Fc $\gamma$ RIIIa binding assay**

Fc $\gamma$ RIIIa binding affinity of SB2 was measured by SPR. Purified Fc $\gamma$ RIIIa (156V/V) was immobilized on a CM5 sensor chip using N-hydroxysuccinimide/N-ethyl-N'-(-3-dimethylamino-propyl) carbodiimide (NHS/EDC). Various concentrations of samples were prepared with HBS-EP buffer and injected into the flow cell for association and dissociation. For regeneration, HBS-EP buffer was injected. Binding affinity was calculated from sensorgrams using the affinity model of the BIA evaluation software.

### **Antibody-dependent cell-mediated cytotoxicity assay**

ADCC assays were performed with a stable mouse cell line that overexpresses human membrane TNF- $\alpha$  on the cell surface (3T3mTNF $\alpha$  cells) as target cells and PBMCs from a healthy donor (Fc $\gamma$ RIIIa 158V/F) as effector cells. Samples were incubated with 3T3mTNF- $\alpha$  cells and PBMCs for 4 hours. Following incubation, the cell plate was incubated with a luminogenic peptide substrate for proteases from dead cells (Cytotox-Glo), and the resulting signal was quantified with a luminometer.

### **Complement-dependent cytotoxicity assay**

The CDC-inducing ability of SB2 was evaluated in an enzyme reaction-based CDC assay. Jurkat-mTNF- $\alpha$  cells were used as target cells, and human serum served as a complement source.

Samples were incubated with Jurkat-mTNF- $\alpha$  cells and human serum. Following incubation, the numbers of viable cells were determined by measuring the luminescence signal induced by cleavage of Cytotox-Glo.

### C1q binding assay

The C1q binding activity of SB2 was measured by a sandwich ELISA. The 96-well MaxiSorp microplates were coated with a dilution series of sample. After blocking, purified human complement protein C1q was added. The binding of C1q to the sample was detected using chicken polyclonal anti-C1q antibody conjugated with HRP and subsequent enzyme reaction by adding TMB solution. Optical density at 450 nm was measured by microplate reader, after adding stop solution.

### Fc $\gamma$ R1a binding assay

Fc $\gamma$ R1a binding activity of SB2 was measured by a competitive inhibition binding assay using TR-FRET. In this assay, Europium-labeled infliximab competes with unlabeled sample for binding to Cy5-labeled Fc $\gamma$ R1a. The procedure was similar to that of TNF- $\alpha$  binding assay.

### Other Fc $\gamma$ R binding assays

Binding affinity of SB2 to other Fc $\gamma$ Rs (Fc $\gamma$ RIIa, Fc $\gamma$ RIIb, and Fc $\gamma$ RIIIb) were measured by SPR. Purified Fc $\gamma$ R protein was immobilized on a CM5 sensor chip using N-hydroxysuccinimide/N-ethyl-N'-(3-dimethylamino-propyl) carbodiimide (NHS/EDC). Various concentrations of samples were prepared with HBS-EP buffer and injected into the flow cell for association and dissociation. For regeneration, HBS-EP buffer was injected. Binding affinity was calculated from sensorgrams using the affinity model of the BIA evaluation software.

### Disclosure of potential conflicts of interest

No potential conflicts of interest were disclosed.

### Acknowledgments

We thank Sandy Field, PhD; Denise Pazano, PharmD; Kelly Schrank, MA, ELIS; and Julia C. Jones, PharmD, PhD, MWC<sup>TM</sup>, of Med Communications, Inc., for their writing and editing assistance.

### Funding

This work was funded by Samsung Bioepis Co., Ltd.

### ORCID

Nayoung Lee  <http://orcid.org/0000-0002-7817-7995>  
 Jongmin Park  <http://orcid.org/0000-0003-3032-3559>  
 Min Jeong  <http://orcid.org/0000-0002-2424-6481>  
 Orlando Jaquez  <http://orcid.org/0000-0002-2885-5081>

### References

- Dorner T, Strand V, Cornes P, Gonçalves J, Gulácsi L, Kay J, Kvien TK, Smolen J, Tanaka Y, Burmester GR. The changing landscape of biosimilars in rheumatology. *Ann Rheum Dis* 2016; 0:1-9; PMID: 26964144; <http://dx.doi.org/10.1136/annrheumdis-2016-209166>
- Gascon P. The evolving role of biosimilars in haematology-oncology: a practical perspective. *Ther Adv Hematol* 2015; 6:267-81; PMID: 26622996; <http://dx.doi.org/10.1177/2040620715613715>
- Niazi SK. Biosimilars and interchangeable biologics: Strategic elements Boca Raton, FL: CRC Press, 2016.
- European Medicines Agency, Committee for Medicinal Products for Human Use. EMA/CHMP/589317/2013. [http://www.ema.europa.eu/docs/en\\_GB/document\\_library/EPAR\\_Public\\_assessment\\_report/human/002576/WC500151486.pdf](http://www.ema.europa.eu/docs/en_GB/document_library/EPAR_Public_assessment_report/human/002576/WC500151486.pdf). Accessed April 30, 2016.
- European Medicines Agency, Committee for Medicinal Products for Human Use. EMA/CHMP/819219/2015. [http://www.ema.europa.eu/docs/en\\_GB/document\\_library/EPAR\\_Public\\_assessment\\_report/human/004007/WC500200380.pdf](http://www.ema.europa.eu/docs/en_GB/document_library/EPAR_Public_assessment_report/human/004007/WC500200380.pdf). Accessed April 30, 2016.
- European Medicines Agency, Committee for Medicinal Products for Human Use. EMA/CHMP/272283/2016. [http://www.ema.europa.eu/docs/en\\_GB/document\\_library/EPAR\\_Public\\_assessment\\_report/human/004020/WC500208358.pdf](http://www.ema.europa.eu/docs/en_GB/document_library/EPAR_Public_assessment_report/human/004020/WC500208358.pdf). Accessed April 30, 2016.
- Weise M, Bielsky MC, De Smet K, Ehmann F, Ekman N, Narayanan G, Heim HK, Heinonen E, Ho K, Thorpe R, et al. Biosimilars-why terminology matters. *Nat Biotechnol* 2011; 29:690-3; PMID:21822237; <http://dx.doi.org/10.1038/nbt.1936>
- Beck A, Wurch T, Bailly C, Corvaia N. Strategies and challenges for the next generation of therapeutic antibodies. *Nat Rev Immunol* 2010; 10:345-52; PMID:20414207; <http://dx.doi.org/10.1038/nri2747>
- US Food and Drug Administration. Title VII—Improving access to innovative medical therapies: Subtitle A—Biologics price competition and innovation. <http://www.fda.gov/downloads/Drugs/GuidanceComplianceRegulatoryInformation/ucm216146.pdf>. Accessed April 30, 2016.
- Cho IH, Lee N, Song D, Jung SY, Bou-Assaf G, Sosic Z, Zhang W, Lyubarskaya Y. Evaluation of the structural, physicochemical, and biological characteristics of SB4, a biosimilar of etanercept [published online ahead of print May 31, 2016]. *mAbs* 2016; 8(6):1136-55; PMID:27246928; <http://dx.doi.org/10.1080/19420862.2016.1193659>
- Knight DM, Trinh H, Le J, Siegel S, Shealy D, McDonough M, Scallon B, Moore MA, Vilcek J, Daddona P. Construction and initial characterization of a mouse-human chimeric anti-TNF antibody. *Mol Immunol* 1993; 30:1443-53; PMID:8232330; [http://dx.doi.org/10.1016/0161-5890\(93\)90106-L](http://dx.doi.org/10.1016/0161-5890(93)90106-L)
- Remicade Prescribing Information (Janssen Biotech, Inc). Available from: <http://www.remicade.com/shared/product/remicade/prescribing-information.pdf>. Accessed April 30, 2016.
- International Conference on Harmonisation of Technical Requirements for Registration of Pharmaceuticals for Human Use. ICH Tripartite Guideline. Specifications: test procedures and acceptance criteria for biotechnological/biological products Q6B. Recommended for adoption on March 10, 1999. <http://www.gmp-compliance.org/guidemgr/files/3-1-17.pdf>. Accessed January 20, 2016.
- US Food and Drug Administration. Guidance for industry: quality considerations in demonstrating biosimilarity of a therapeutic protein product to a reference product. <http://www.fda.gov/downloads/drugs/guidancecomplianceregulatoryinformation/guidances/ucm291134.pdf>. Published April 2015 Accessed January 20, 2016.
- Schiestl M, Stangler T, Torella C, Cepeljnik T, Toll H, Grau R. Acceptable changes in quality attributes of glycosylated biopharmaceuticals. *Nat Biotechnol* 2011; 29:310-2; PMID:21478841; <http://dx.doi.org/10.1038/nbt.1839>
- European Medicines Agency, Committee for Medicinal Products for Human Use. Guideline on similar biological medicinal products containing biotechnology-derived proteins as active substance: quality issues (revision 1). [http://www.ema.europa.eu/docs/en\\_GB/document\\_library/Scientific\\_guideline/2014/06/WC500167838.pdf](http://www.ema.europa.eu/docs/en_GB/document_library/Scientific_guideline/2014/06/WC500167838.pdf). Updated May 22, 2014 Accessed February 5, 2016.
- European Medicines Agency, Committee for Medicinal Products for Human Use. Guideline on similar biological medicinal products [Internet]. London, UK: European Medicines Agency; [Adopted on October 23, 2014; cited February 5, 2016]. Available

- from: [http://www.ema.europa.eu/docs/en\\_GB/document\\_library/Scientific\\_guideline/2014/10/WC500176768.pdf](http://www.ema.europa.eu/docs/en_GB/document_library/Scientific_guideline/2014/10/WC500176768.pdf)
18. Chamberlain J. Biosimilars and analytical challenges. *Pharm J* 2009. <http://www.pharmaceutical-journal.com/news-and-analysis/news/biosimilars-and-analytical-challenges/10971836.article>. Accessed April 30, 2016.
  19. Zhong X, Wright JF. Biological insights into therapeutic protein modifications throughout trafficking and their biopharmaceutical applications. *Int J Cell Biol* 2013; 2013:273086; PMID:23690780; <http://dx.doi.org/10.1155/2013/273086>. Accessed April 30, 2016.
  20. Wang X, Li O, Davies M. Higher-order structure comparability: case studies of biosimilar monoclonal antibodies. *Bioprocess Int* 2014; 12:32-47.
  21. Houde D, Berkowitz SA, Engen JR. The utility of hydrogen deuterium exchange mass spectrometry in biopharmaceutical comparability studies. *J Pharm Sci* 2011; 100:2071-86; PMID:21491437; <http://dx.doi.org/10.1002/jps.22432>
  22. Wang X, Li Q, Davis M. Development of antibody arrays for monoclonal antibody higher order structure analysis. *Front Pharmacol* 2013; 4 (Article 103):1-8; PMID:23970865; <http://dx.doi.org/10.3389/fphar.2013.00103>
  23. US Food and Drug Administration. Guidance for industry: immunogenicity assessment for therapeutic protein products. <http://www.fda.gov/downloads/drugs/guidancecomplianceregulatoryinformation/guidances/ucm338856.pdf>. Published August 2014 Accessed Apr 30, 2016.
  24. Rosenberg AS. Effects of protein aggregates: an immunologic perspective. *AAPS J* 2006; 8:E501-7; PMID:17025268; <http://dx.doi.org/10.1208/aapsj080359>
  25. Pilo JS. A critical review of methods for size characterization of non-particulate protein aggregates. *Current Pharm Biotechnol* 2009; 10:359-72; PMID:19519411; <http://dx.doi.org/10.2174/138920109788488815>
  26. Putnam WS, Prabhu S, Zheng Y, Subramanyam M, Wang YM. Pharmacokinetic, pharmacodynamics and immunogenicity comparability assessment strategies for monoclonal antibodies. *Trends in Biotechnol* 2010; 28(10):509-516; PMID:20691488; <http://dx.doi.org/10.1016/j.tibtech.2010.07.001>
  27. Shields RL, Lai J, Keck R, O'Connell LY, Hong K, Meng YG, Weikert SH, Presta LG. Lack of fucose on human IgG1 N-linked oligosaccharide improves binding to human Fc RIII and antibody-dependent cellular toxicity. *J Biol Chem* 2002; 277:26733-40; PMID:11986321; <http://dx.doi.org/10.1074/jbc.M202069200>
  28. Raju TS. Terminal sugars of Fc glycans influence antibody effector functions of IgGs. *Curr Opin Immunol* 2008; 20:4718; PMID:18606225; <http://dx.doi.org/10.1016/j.coi.2008.06.007>
  29. Butler M, Spearman M. The choice of mammalian cell host and possibilities for glycosylation engineering. *Curr Opin Immunol* 2014; 30:107-112; PMID:25005678; <http://dx.doi.org/10.1016/j.copbio.2014.06.010>
  30. van Beers MMC, Bardor M. Minimizing immunogenicity of biopharmaceuticals by controlling critical quality attributes of proteins. *Biotechnol J* 2012; 7:1-12; PMID:23027660; <http://dx.doi.org/10.1002/biot.201200065>
  31. Flynn GC, Chen X, Liu YD, Shah B, Zhang Z. Naturally occurring glycan forms of human immunoglobulins G1 and G2. *Mol Immunol* 2010; 47:2074-82; PMID:2044501; <http://dx.doi.org/10.1016/j.molimm.2010.04.006>
  32. Scallan BJ, Tam SH, McCarthy SG, Cai AN, Raju TS. Higher levels of sialylated Fc glycans in immunoglobulin G molecules can adversely impact functionality. *Mol Immunol* 2006; 44:1524-34; PMID:17045339; <http://dx.doi.org/10.1016/j.molimm.2006.09.005>
  33. Kaneko Y, Nimmerjahn F, Ravetch JV. Anti-inflammatory activity of immunoglobulin G resulting from Fc sialylation. *Science* 2006; 313:670-3; PMID:16888140; <http://dx.doi.org/10.1126/science.1129594>
  34. Liu H, Ponniah G, Zhang HM, Nowak C, Neill A, Gonzalez-Lopez N, Patel R, Cheng G, Kita AZ, Andrien B. In vitro and in vivo modifications of recombinant and human IgG antibodies. *mAbs* 2014; 6:1145-1154; PMID:29883; <http://dx.doi.org/10.4161/mabs>
  35. Johnson KA, Paisley-Flango K, Tangarone BS, Porter TJ, Rouse JC. Cation exchange-HPLC and mass spectrometry reveal C-terminal amidation of an IgG1 heavy chain. *Anal Biochem* 2007; 360:75-83; PMID:17113563; <http://dx.doi.org/10.1016/j.ab.2006.10.012>
  36. Bradbury AF, Smyth DG. Peptide amidation. *Trends Biochem Sci* 1991; 16:112-5; PMID:2057999; [http://dx.doi.org/10.1016/0968-0004\(91\)90044-V](http://dx.doi.org/10.1016/0968-0004(91)90044-V)
  37. Lügering A, Schmidt M, Lügering N, Pauels H-G, Domschke W, Kucharzik T. Infliximab induces apoptosis in monocytes from patients with chronic active Crohn's disease by using a caspase-dependent pathway. *Gastroenterology* 2001; 121:1145-57; PMID:11677207; <http://dx.doi.org/10.1053/gast.2001.28702>
  38. Horicuchi T, Mitoma H, Harashima S, Tsukamoto H, Shimoda T. Transmembrane TNF- $\alpha$ : structure, function and interaction with anti-TNF agents. *Rheumatology* 2010; 49:1215-28; PMID:20194223; <http://dx.doi.org/10.1093/rheumatology/keq031>
  39. Peppelenbosch MP, van Deventer SJ. T cell apoptosis and inflammatory bowel disease. *Gut* 2004; 53(11):1556-58; PMID:15479669; <http://dx.doi.org/10.1136/gut.2004.040824>
  40. Hove T, Van Montfrans CV, Peppelenbosch MP, van Deventer SJH. Infliximab treatment induces apoptosis of lamina propria T lymphocytes in Crohn's disease. *Gut* 2002; 50:206-11; PMID:11788561; <http://dx.doi.org/10.1136/gut.50.2.206>
  41. Di Sabatino A, Ciccocioppo R, Cinque B, Millimaggi D, Morera R, Ricevuti L, Cifone MG, Corazza GR. Defective mucosal T cell death is sustainably reverted by infliximab in a caspase dependent pathway in Crohn's disease. *Gut* 2004; 53:70-7; PMID:14684579; <http://dx.doi.org/10.1136/gut.53.1.70>
  42. Suzuki T, Ishii-Watabe A, Tada M, Kobayashi T, Kanayasu-Toyoda T, Kawanishi T, Yamaguchi T. Importance of neonatal FcR in regulating the serum half-life of therapeutic proteins containing the Fc domain of human IgG1: a comparative study of the affinity of monoclonal antibodies and Fc-fusion proteins to human neonatal FcR. *J Immunol* 2010; 184:1968-76; PMID:20083659; <http://dx.doi.org/10.4049/jimmunol.0903296>
  43. Hermeling S, Crommelin DJ, Schellekens H, Jiskoot W. Structure-immunogenicity relationships of therapeutic proteins. *Pharm Res* 2004; 21:897-903; PMID:15212151; <http://dx.doi.org/10.1023/B:PHAM.0000029275.41323.a6>
  44. Singh SK. Impact of product-related factors on immunogenicity of biotherapeutics. *J Pharm Sci* 2011; 100:354-87; PMID:20740683; <http://dx.doi.org/10.1002/jps.22276>
  45. Li CH, Nguyen X, Narhi L, Chemmalil L, Towers E, Muzammil S, Gabrielson J, Jiang Y. Applications of circular dichroism (CD) for structural analysis of proteins: qualification of near- and far-UV CD for protein higher-order structural analysis. *J Pharm Sci* 2011; 100:4642-54; PMID:21732370; <http://dx.doi.org/10.1002/jps.22695>
  46. Garidel P, Hegyi M, Bassarab S, Weichel M. A rapid, sensitive and economical assessment of monoclonal antibody conformational stability by intrinsic tryptophan fluorescence spectroscopy. *Biotechnol J* 2008; 3:1201-11; PMID:18702089; <http://dx.doi.org/10.1002/biot.200800091>